Am J Physiol Heart Circ Physiol 316: H647–H663, 2019.
First published January 11, 2019; doi:10.1152/ajpheart.00090.2018.

RESEARCH ARTICLE | *Vascular Biology and Microcirculation*

Role of matrix metalloproteinases and histone deacetylase in oxidative stress-induced degradation of the endothelial glycocalyx

Mohamed M. Ali,[1,2] Abeer M. Mahmoud,[1,2] Elizabeth Le Master,[3] Irena Levitan,[3] and Shane A. Phillips[1,2,4]

[1]*Department of Physical Therapy, College of Applied Health Sciences, University of Illinois at Chicago, Chicago, Illinois;* [2]*Integrative Physiology Laboratory, College of Applied Health Sciences, University of Illinois at Chicago, Chicago, Illinois;* [3]*Division of Pulmonary and Critical Care, Department of Medicine, University of Illinois at Chicago, Chicago, Illinois; and* [4]*Division of Endocrinology, Diabetes, and Metabolism, Department of Medicine, University of Illinois at Chicago, Chicago, Illinois*

Submitted 2 February 2018; accepted in final form 6 November 2018

Ali MM, Mahmoud AM, Le Master E, Levitan I, Phillips SA. Role of matrix metalloproteinases and histone deacetylase in oxidative stress-induced degradation of the endothelial glycocalyx. *Am J Physiol Heart Circ Physiol* 316: H647–H663, 2019. First published January 11, 2019; doi:10.1152/ajpheart.00090.2018.—The glycocalyx is crucial for normal endothelial function. It also tethers extracellular superoxide dismutase (SOD3), which protects the endothelium against oxidative damage. Proteolytic enzymes [matrix metalloproteinases (MMPs)] are capable of disrupting endothelial cell surface proteins, such as syndecans, resulting in derangements of the endothelial glycocalyx. We sought to test the role of MMPs in oxidative stress-mediated disruption of the endothelial glycocalyx and examine the effect of pharmacological inhibition of MMPs on mitigating this detrimental effect. We also examined the role of histone deacetylase (HDAC) in the oxidative stress-mediated MMP induction and glycocalyx remodeling. Oxidative stress was experimentally induced in human adipose microvascular endothelial cells using H_2O_2 and buthionine sulfoximine in the presence and absence of potent MMP and HDAC inhibitors. H_2O_2 and buthionine sulfoximine resulted in a notable loss of the endothelial glycocalyx; they also increased the expression and proteolytic activity of MMP-2 and MMP-9 and subsequently increased the shedding of syndecan-1 and SOD3 from the endothelial cell surface. MMP upregulation was accompanied by a decline in mRNA and protein levels of their inhibitors, tissue inhibitors of metalloproteinase (TIMPs; TIMP-1 and TIMP-3). Furthermore, oxidative stress induced HDAC activity. Inhibition of MMPs and HDAC reversed syndecan-1 and SOD3 shedding and maintained endothelial glycocalyx integrity. HDAC inhibition increased TIMP expression and reduced MMP expression and activity in endothelial cells. Our findings shed light on MMPs and HDAC as therapeutically targetable mechanisms in oxidative stress-induced glycocalyx remodeling.

NEW & NOTEWORTHY Oxidative stress, a hallmark of many diseases, damages the endothelial glycocalyx, resulting in vascular dysfunction. Studying the mechanistic link between oxidative stress and endothelial glycocalyx derangements might help discover new therapeutic targets to preserve vascular function. In this study, we investigated the involvement of matrix metalloproteinases and histone deacetylase in oxidative stress-induced endothelial glycocalyx degradation.

Address for reprint requests and other correspondence: S. A. Phillips, Dept. of Physical Therapy, Univ. of Illinois at Chicago, 1919 W. Taylor St. (AHSB), Rm. 746 (M/C 898), Chicago, IL 60612 (e-mail: shanep@uic.edu).

endothelial glycocalyx; histone deacetylase; matrix metalloproteinase; oxidative stress; superoxide dismutase

INTRODUCTION

The endothelial glycocalyx is a thin layer of proteoglycans anchored to the endothelial cell surface and comprised mainly of sugar moieties termed glycosaminoglycans (GAGs) that are highly sulfated forms of heparin, chondroitin, and dermatan chains conjugated to core proteins, mainly syndecans and glypicans (59). Syndecans are the primary heparan sulfate proteoglycans (HSPGs) expressed on the endothelial cell surface, and their circulating levels have been associated with heart failure, cardiomyopathy, and other cardiovascular conditions (5, 20, 53). Endothelial HSPGs contribute to vascular barrier function, mechanotransduction of shear stress and flow-mediated vascular responses, adhesion of leukocytes, and inflammation (6, 15, 39). Moreover, HSPGs support an antioxidant and antithrombotic function by harboring extracellular antioxidant enzymes and antithrombotic factors (6). Given the importance of the endothelial glycocalyx in facilitating the initial inflammatory response in the vascular wall in addition to its role in vascular endothelial function, a deeper understanding of the factors playing role in the structural and functional integrity of the endothelial glycocalyx is of great translational value.

Matrix metalloproteinases (MMPs) are a group of zinc-containing enzymes that are responsible for degradation of the extracellular matrix (ECM) and connective tissue proteins (17, 56). MMPs are produced by endothelial cells and play a critical role in vascular remodeling. A growing body of evidence supports the involvement of dysregulated MMPs in cardiovascular diseases (CVDs) including atherosclerosis, aneurysms, and hypertension. Atherosclerotic plaques showed increased expression of MMP-1, MMP-2, and MMP-9 as well as a disturbed ratio of MMPs and tissue inhibitors of metalloproteinase (TIMPs) (3, 23). Patients with acute myocardial infarction, unstable angina, and hypertension exhibited higher levels of circulating MMPs such as MMP-2 and MMP-9 relative to healthy individuals (11, 22). Patients with hypertension also showed higher serum levels of TIMP-1 and the MMP-1-to-TIMP-1 ratio compared with normotensive control individuals

(27). These findings suggest that matrix remodeling via MMPs may contribute to CVD and that MMPs may be an important therapeutic target. Also, these findings raise the possibility that pharmacological agents or small molecules with MMP-regulating properties may serve as preventive or adjuvant therapeutic agents for patients with CVD.

Studies have shown that inflammation and oxidative stress are hallmarks of CVD (4). Increased reactive oxygen species (ROS) production is a known promoting factor for the development of atherosclerosis, hypertension, and other vascular lesions. However, the mechanistic link between ROS production and endothelial glycocalyx remodeling and the involvement of MMPs in this pathway remain unclear. Driven by this clinical significance, we sought to confirm the role of MMPs in mediating the effect of experimentally induced oxidative stress on disrupting the endothelial glycocalyx and to examine if pharmacological inhibition of MMPs may be protective against the oxidative stress-elicited disruption of the endothelial glycocalyx. Oxidative stress has been shown to modulate histone deacetylase (HDAC) activity; however, the available data are inconsistent, and it is not clear whether HDAC activity increases or decreases in response to redox signaling (8, 19, 42). HDAC is a known modulator of a myriad of inflammatory and tissue remodeling genes. Yet, its role in microvascular glycocalyx integrity under conditions of oxidative stress is not clear. Therefore, in the present study, we sought to explore the role of HDAC in modifying MMP/TIMP gene expression and glycocalyx structure in microvascular endothelial cells under conditions of oxidative stress.

MATERIALS AND METHODS

Chemicals and reagents. Buthionine sulfoximine (BSO), H_2O_2, trichostatin (TSA), and marimastat were purchased from Sigma-Aldrich (St. Louis, MO). Suberoylanilide hydroxamic acid (SAHA) and 2-[(4-phenoxyphenylsulfonyl)methyl]thiirane (SB-3CT) were purchased from Santa Cruz Biotechnology (Dallas, TX).

Antibodies and DNA primers. Primary monoclonal antibodies against syndecan-1, syndecan-2, syndecan-3, glypican, MMP-2, MMP-2, MMP-9, and extracellular superoxide dismutase (SOD3) were purchased from Santa Cruz Biotechnology. TIMP-1, TIMP-3, and β-actin antibodies were purchased from Cell Signaling (Danvers, MA). Primers for MMP-1, MMP-2, MMP-3, TIMP-1, TIMP-3, SOD3, syndecan-1, syndecan-2, and syendecan-3 were designed using online Primer3 software (http://primer3.ut.ee/) and validated for efficiency.

Culture of human adipose microvascular endothelial cells. Human adipose microvascular endothelial cells (HAMECs) were obtained from ScienCell Research Laboratories (Rockville, MD), and *passages 1−5* were used to perform the experiments. Cells were maintained in phenol red-free ECM media with L-glutamine supplemented with 5% FBS, 100 IU/ml penicillin, and 100 μg/ml streptomycin. Experiments were performed using *passages 2−6*.

Cell viability assay. HAMECs were assayed for viability by incubation with calcein AM, which is a cell-permeant cell viability dye. Calcein AM is a substrate of intracellular esterases that is converted into green fluorescent calcein dye after hydrolysis by intracellular esterases in viable cells (26). HAMECs were labeled with calcein AM and then treated with H_2O_2 for up to 6 h. Cell cultures were dissociated from the culture dish and suspended in PBS for flow cytometric analysis of fluorescence.

Flow cytometric analysis. Cells were seeded for culture into six-well plates and maintained in ECM media until reaching 90–100% confluence. Cells were incubated with H_2O_2 for 1, 2, or 4 h. Treated cells were washed in PBS and stained for wheat germ agglutinin (WGA; Invitrogen) to label GAG moieties on the glycocalyx. Cells were collected using nonenzymatic cell dissociation buffer and then analyzed using the BD accuri C6 flow cytometer and the bundled software package.

Glycocalyx fluorescence microscopy imaging experiments. Fluorescence microscopy was used for qualitative or semiquantitative analysis of glycocalyx density on the endothelial cell surface. Cells were seeded for culture into six-well plates and maintained in ECM media until reaching 90–100% confluence. Cells were incubated with H_2O_2 or BSO in the presence or absence of marimastat (50 μM), SB-3CT (100 nM), SAHA (5 μM), or TSA (1 μM) for 1, 2, or 4 h. Treated cells were washed in PBS and incubated in WGA (25) Alexa Fluor 594 (Invitrogen) at a concentration of 3 μg/ml in PBS to label GAG moieties on the glycocalyx. Fluorescent-labeled HAMECs were then imaged using an inverted fluorescence microscope (excitation: 590 nm and emission: 617 nm, Diaphot, Nikon) equipped with a sCMOS camera (Tucsen ICE1.3) under control of the bundled imaging software. Image analysis functions including color histograms were performed on fluorescence images using the ImageJ software package (47).

Real-time PCR. Total RNA was extracted from each sample using the RNeasy mini kit (Qiagen, Germantown, MD). The isolated RNA quantity was estimated by spectrophotometric measurement of absorbance at 260 and 280 nm. From each sample, 5 μg of the isolated total RNA were reverse transcribed into cDNA using SuperScript RT III (Invitrogen). mRNA expression was determined by real-time RT-PCR using the SYBR Green Assay standard protocol and Agilent Mx3005P qPCR System (Agilent Technologies, Santa Clara, CA). Specific primers for each gene were designed (Table 1). GAPDH was used as the internal control. The normalized expression ratio of the target genes was calculated using the $2^{-\Delta\Delta C_t}$ (Livak) method from theshold cycles (C_t) generated by the real-time RT-PCR. Reactions were carried out in triplicate, and results show three independent experiments.

Western blot analysis. For Western blot analysis, total protein was isolated from treated cells using 1× cell lysis buffer (Cell Signaling). To normalize protein loading, each sample protein concentration was first measured using the Bio-Rad Protein Assay kit (Bio-Rad Laboratories, Hercules, CA) at 595 nm with a microplate reader. Twenty-five micrograms of protein per lane were resolved by a NuPAGE 4–12% bis-Tris gel (Invitrogen) and transferred to PVDF membranes. The immunoblot was incubated with primary antibodies overnight at 4°C and then with infrared IRDye-labeled secondary antibodies (LI-COR Biosciences, Lincoln, NE) for 1 h at room temperature, protected from light. Blots were washed with Tris-buffered saline + 0.1% Tween 20, dried for 1 h at room temperature, and then scanned in the appropriate channel (700 nm for IRDye680 antibodies and 800 nm for IRDye800 antibodies) using an Odyssey CLx infrared imaging system. β-Actin was used as a loading control. Images were then quantified using Image Studio (version 4.0, LI-COR) to calculate the intensity of the bands of the protein of interest relative to the β-actin housekeeping gene from three independent experiments.

Immunoprecipitation. Immunoprecipitation of syndecan-1 or SOD3 was performed from cell culture media using Dynabeads protein G magnetic beads (Invitrogen, Life Technologies). Primary antibody for each protein was incubated with Dynabeads for 1 h at room temperature, and the complex was then incubated with 2 ml of the cell culture media overnight at 4ºC. Protein was isolated by elution using sample buffer with a reducing agent for downstream analysis using Western blots.

HDAC activity assay. Cells were seeded in a 96-well plate at a density of 5×10^4 cells/well in 100 μl of culture medium until they reached 80% confluence. Cells were then incubated with H_2O_2 in the presence or absence of marimastat (50 μM) or TSA (1 μM) for 4 h in a CO_2 incubator at 37°C. HDAC activity was measured using the HDAC Cell-Based Activity Assay Kit (Cayman Chemical, Ann Arbor, MI) following the vendor's protocol. Briefly, the culture medium

Table 1. *Sequences of primers used for real-time PCR*

Gene Name	Primer Sequence	Melting Temperature, °C	Product Size, bp
MMP-1			
Forward primer	5′-AAAATTACACGCCAGATTTGCC-3′	60	82
Reverse primer	5′-GGTGTGACATTACTCCAGAGTTG-3′	60.5	
MMP-2			
Forward primer	5′-TACAGGATCATTGGCTACACACC-3′	61.7	90
Reverse primer	5′-GGTCACATCGCTCCAGACT-3′	61.1	
MMP-9			
Forward primer	5′-TGTACCGCTATGGTTACACTCG-3′	61.5	97
Reverse primer	5′-GGCAGGGACAGTTGCTTCT-3′	61.9	
TIMP-1			
Forward primer	5′-CTTCTGCAATTCCGACCTCGT-3′	62.4	79
Reverse primer	5′-ACGCTGGTATAAGGTGGTCTG-3′	61.3	
TIMP-3			
Forward primer	5′-CATGTGCAGTACATCCATACGG-3′	60.8	100
Reverse primer	5′-CATCATAGACGCGACCTGTCA-3′	61.6	
Syndecan-1			
Forward primer	5′-CTGCCGCAAATTGTGGCTAC-3′	62.3	81
Reverse primer	5′-TGAGCCGGAGAAGTTGTCAGA-3′	62.9	
Syndecan-2			
Forward primer	5′-TTGACAACAGCTCCATTGAAGAA-3′	60.4	110
Reverse primer	5′-CAGCTCTGGACTCTCTACATCC-3′	61	
Syndecan-1			
Forward primer	5′-TGGCGCAGTGAGAACTTCG-3′	62.6	96
Reverse primer	5′-CCCCGAGTAGAGGTCATCCAG-3′	62.9	

MMP, matrix metalloproteinase; TIMP, tissue inhibitor of metalloproteinase.

was aspirated, and cells were washed with diluted assay buffer. HDAC reactions were initiated by the addition of 10 μl diluted HDAC substrate/90 μl culture medium to each well, and cells were incubated at 37°C. Two hours later, 50 μl of the Lysis/Developer Solution were added to each well, and cells were incubated for 15 min. Human recombinant HDAC1- or TSA-treated cells were used as positive and negative controls, respectively. Each sample was assayed in the presence and absence of the HDAC inhibitor to allow for the correction of HDAC-independent fluorescence. HDAC deacetylated standards were used to generate a standard curve (concentration ranged from 0 to 168 μM), which was used to calculate HDAC activity in the test samples. The fluorescence intensity of each well (excitation: 340–360 nm and emission: 440–460 nm) was determined using a SpectraMax M Series Multi-Mode Microplate Reader (Molecular Devices, Fully Vale, CA). TSA sample fluorescence was subtracted from non-TSA sample fluorescence to yield the corrected sample fluorescence. HDAC activity was then calculated using the following equation obtained from the linear regression of the standard curve, substituting corrected fluorescence values for each sample: HDAC activity (in $nmol \cdot min^{-1} \cdot ml^{-1}$) = [corrected sample fluorescence − (*y*-intercept)/slope]/15 min.

Zymography. Ready Gel 10% zymogram gels with gelatin and collagen (Abcam, Cambridge, MA) were used to test MMP activity in conditioned media following the vendor's zymography protocol. HAMECs were cultured in a six-well plate until reaching 70–80% confluency. Cells were incubated with H_2O_2 or BSO in the presence or absence of marimastat (50 μM) or TSA (1 μM) for 4 h. Conditioned media were collected and centrifuged to eliminate dead cells and then adjusted in all samples to the same protein concentration. Samples were mixed with SDS-PAGE loading buffer without a reducing agent and subjected to electrophoresis at room temperature. After electrophoresis, gels were soaked for 1 h in washing buffer that removes SDS [2.5% Triton X-100, 50 mM Tris·HCl (pH 7.5), 5 mM $CaCl_2$, and 1 μM $ZnCl_2$], after which gels were incubated in gelatinase reactivation buffer [1% Triton X-100, 50 mM Tris·HCl (pH 7.5), 5 mM $CaCl_2$, and 1 μM $ZnCl_2$] at 37°C overnight. Gels were stained with Coomassie blue dye for 1 h followed by destaining until proteolytic activities were visualized by clear zones against a dark blue background indicating lysis of gelatin. Quantification of the proteinase activities, which were expressed as arbitrary units, was performed using the ImageJ software package on scanned images of the gels.

Glycocalyx biomechanical analysis experiments using an atomic force microscopy atomic force microscope. The atomic force microscope (AFM) is a scanning probe microscope designed to measure local properties such as surface biomechanical properties including height, friction, texture, and stiffness with a probe. AFM, normally used for the purpose of imaging, can also provide structural information about the cell. The probe used in AFM consists of a fine pyramidal tip attached to a cantilever that flexes as the tip is pushed into the sample surface. By measuring the flexure in the cantilever with the reflection of a laser, it is possible to calculate the upward force acting at the tip.

AFM has been frequently used to measure the mechanical stiffness of endothelial cells using indentation techniques that involve the use of a sharp tip that indents the cell membrane and exerts pressure on the membrane and cytoskeleton. AFM was used together with finite-element analysis to show the increase in elastic moduli for bovine endothelial cells exposed to shear stress (44). Live cell elasticity was measured with a Novascan AFM (Novascan Technologies, Ames, IA) mounted on an inverted TE-2000 Nikon microscope. Soft silicon nitride cantilevers (100 μm long, Veeco, Santa Barbara, CA) were calibrated by the thermal fluctuation method in air, with a typical spring constant value of 0.12 N/m. Borosilicate glass beads (10 μm in diameter) glued onto the cantilever served as spherical cell indenters. Distribution of the indenting load over several-micrometer area allows removing mechanical spatial heterogeneity of fibrous cell cytoskeleton according to the method previously described by Titushkin and Cho (54).

Cultures of HAMEC monolayers that were at least 60% confluent with normal morphology were mechanically probed with AFM; clusters of adjacent cells were probed while avoiding the cell's perinuclear region. To obtain a force curve, the cantilever descended toward each measured cell at a velocity of ~2 μm/s until a trigger force of 3 nN was reached and then retracted. To minimize the effect of the glass substrate on the cell elasticity measurements, we used an indentation depth up to 500 nm (~10–15% of the average cell height) for data analysis. A total of 30–40 cells of each type and experimental condition were used, with ~15 force-distance curves acquired from

each cell. The force-distance curves were collected and analyzed according to the Hertz model as described in RESULTS (see Fig. 9), which relates the loading force (F) with the indentation depth (δ) by fitting the Hertz model to the experimental force curve with a standard least-squares minimization algorithm yielded the local apparent elastic modulus (*E*). The average Young's modulus for each cell type and experimental condition was calculated and subjected to a *t*-test at the level of 0.05.

Statistical analysis. Data are expressed as means ± SE. Data were analyzed using Student's *t*-test or one-way ANOVA when there were more than two comparisons followed by a post hoc test as appropriate. $P < 0.05$ was considered significant.

RESULTS

Prolonged exposure to endogenously or exogenously induced oxidative stress elicits degradation of the glycocalyx. To determine the effect of oxidative stress on matrix remodeling in endothelial cells, we applied two approaches: *1*) exogenously induced oxidative stress using H_2O_2 (2×10^{-4} mol/l) and *2*) endogenously induced oxidative stress using BSO (10^{-3} mol/l), which has been shown to reduce levels of intracellular glutathione, leading to an abundance of free superoxide radicals and subsequently elevated oxidative stress (52). HAMECs were treated with H_2O_2 or BSO for 1−6 h, after which cell viability was evaluated by a calcein AM cell viability assay showing no signs of toxicity for this dose and duration of treatment (Fig. 1*A*). Measuring the glycocalyx density using flow cytometric analysis of WGA-stained cells revealed significant reductions in the WGA signal in HAMECs treated with H_2O_2 compared with untreated cells (Fig. 1, *B* and *C*). These findings were visually confirmed via fluorescence microscopic imaging of WGA-labeled endothelial cells that demonstrated notable loss of endothelial surface HSPG moieties of the glycocalyx in HAMECs after 4 h of incubation with H_2O_2 compared with control (Fig. 1, *D* and *E*).

Oxidative stress induces shedding of syndecan-1 from the endothelial cell surface. Syndecan-1 is a core protein that is expressed on the endothelial cell surface and tethers HSPG moieties. To test the hypothesis that syndecan shedding is a major contributor to the loss of HSPGs and subsequently the attenuated glycocalyx in oxidative stress, we measured protein levels of syndecan-1 in cell lysates and cell culturing medium under conditions of oxidative stress. Our data showed that inducing oxidative stress using H_2O_2 and BSO decreased protein levels of syndecan-1 by three- and five-fold, respectively, in HAMEC cell lysates compared with baseline levels (Fig. 2*A*). We also measured levels of syndecan-1 in the cell culture media via immunoprecipitation. Our results showed that syndecan-1 was detected in cell

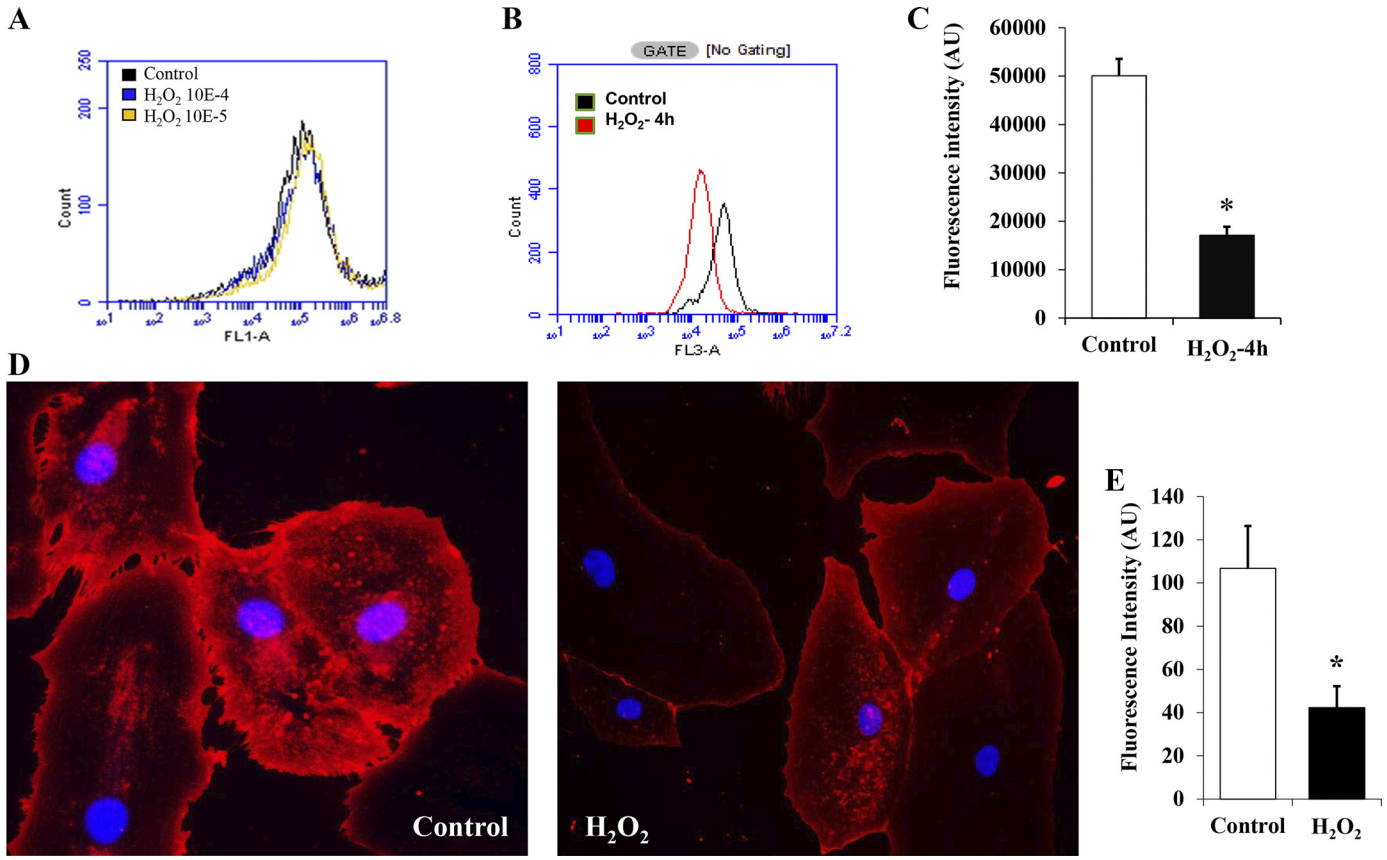

Fig. 1. Effects of H_2O_2 treatment on viability and glycocalyx integrity in human adipose microvascular endothelial cells (HAMECs). *A*: cells were treated with H_2O_2 (2×10^{-4} and 2×10^{-5} mol/l) for 6 h and stained with viability detection stain (calcein AM). The signal was then quantified using flow cytometry. *B* and *C*: quantification of the wheat germ agglutinin (WGA) signal in untreated cells and cells treated with H_2O_2 using flow cytometry. *D* and *E*: fluorescent microscope image (*D*) and fluorescent signal quantified by ImageJ software (*E*) of untreated control cells and cells treated with H_2O_2 (2×10^{-4} mol/l) for 4 h after being labeled with fluorescent WGA. AU, arbitrary units. All graphic presentations are of the mean log of 3 independent experiments (triplicates for each group in each experiment) ± SD. *$P < 0.05$ for comparisons with control.

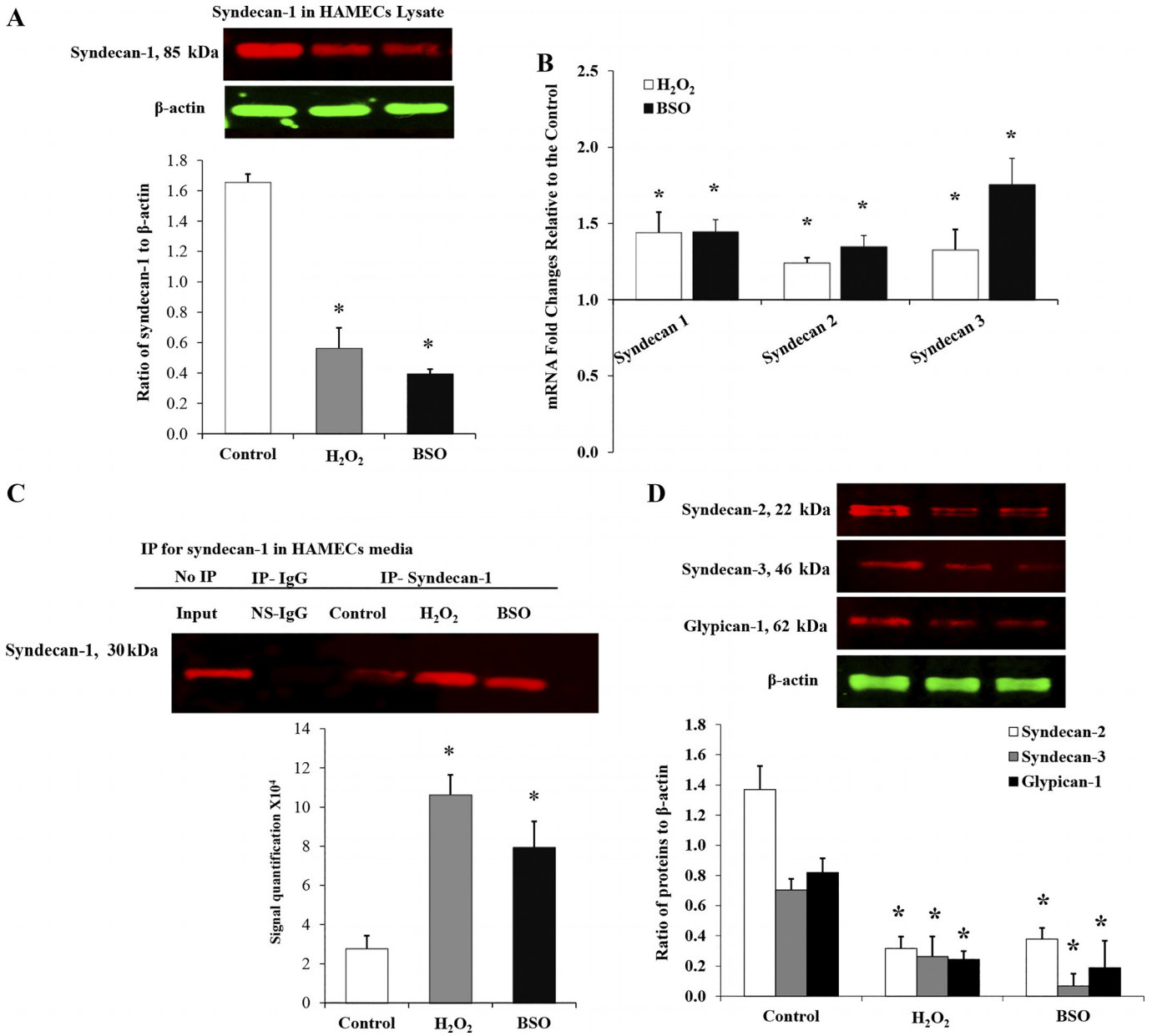

Fig. 2. Effects of oxidative stress on cellular and shed fractions of syndecan-1 in human adipose microvascular endothelial cells (HAMECs). Cells were treated with H_2O_2 (2×10^{-4} mol/l) or buthionine sulfoximine (BSO; 10^{-3} mol/l) for 4 h. *A*: Western blot analysis and signal relative intensity quantification of syndecan-1 protein expression in HAMECs. *B*: mRNA levels of syndecan-1, syndecan-2, and syndecan-3 measured by real-time PCR. Results represent fold changes relative to the untreated control from 3 independent experiments. Western blot analysis of shed syndecan-1 in HAMEC cell culture media is shown; conditioned media were immunoprecipitated (IP) with syndecan-1 antibody or rabbit IgG as a control for nonspecific IgG (NS-IgG) and immunoblotted for syndecan-1. *C*: media of untreated cells were used as a negative control, and media before IP were used to demonstrate that protein bands correspond to the expected molecular weight. *D*: Western blot analysis and signal relative intensity quantification of syndecan-2, syndecan-3, and glypican-1 protein expression in HAMECs. Results represent means ± SD of 3 independent experiments (triplicates for each group in each experiment). *$P < 0.05$ for comparisons with control.

culture media at very low basal levels and lower molecular weight (around 30 vs. 85 kDa in total cell lysate) suggesting that the shed syndecan-1 is the extracellular domain of the protein. This assumption is supported by a previous study by Endo et al. (12), who reported a major digestion product of ~25 kDa for syndecan-1 recombinant protein (full-length) when incubated with MMPs. Treatment with H_2O_2 or BSO increased syndecan-1 in the media by approximately three- to four-fold relative to basal levels (Fig. 2*C*). These data indicate that the oxidative stress-mediated reduction of syndecan-1 is caused by shedding of syndecan-1 protein from the endothelial cell surface and its release in cell culture media. We further assessed the expression of other proteoglycans, syndecan-2, syndecan-3, and glypican-1, that showed similar patterns to syndecan-1 (Fig. 2*D*). In contrast, mRNA levels of syndecan-1, syndecan-2, and syndecan-3 increased (30–70%) in response to oxidative stress, which might indicate a compensatory mechanism to the decreased protein levels (Fig. 2*B*).

Oxidative stress modifies MMP expression and activity in endothelial cells. To investigate the role of MMPs in oxidative stress-induced shedding of syndecan-1 in endothelial cells, we measured MMP expression and activity in oxidatively challenged HAMECs. We also investigated the effect of inhibition of MMP activity using marimastat, a broad-spectrum MMP inhibitor (10). Cells were treated with H_2O_2 or BSO for 2–4 h followed by analysis of MMP (MMP-1, MMP-2, and MMP-9) mRNA and protein expression. Conditioned media were collected and analyzed for MMP-2 and MMP-9 activity via gel zymography. Gelatin-lytic bands at 92 kDa (pro-MMP-9), 83 kDa (MMP-9), 72 kDa (pro-MMP-2), and 62 kDa (MMP-2) are shown in Fig. 3*A*, and their internal control protein (β-actin) was also analyzed by Western blot analysis. After H_2O_2 and BSO treatment, pro-MMP-9, MMP-9, pro-MMP-2, and MMP-2 activities in endothelial cells increased one- to twofold relative to control and was significantly attenuated by marimastat (Fig. 3, *A* and *B*). Accordingly, marimastat was used in the rest of our experiments to test the effect of inhibition of oxidative stress-induced MMP activity on other outcomes such as syndecan-1 shedding, glycocalyx attenuation, and endothelial cell stiffness.

Oxidative stress induced mRNA levels of MMP-1, MMP-2, and MMP-9 by ~1.5- to 3-fold compared with control (Fig. 3*C*) and increased protein levels by 70% and 85% and 3.5-fold, respectively (Fig. 3*D*). Yet, these effects were not changed by coincubation with marimastat, which is not surprising since its effect is mainly on MMP enzymatic activity rather than expression (3, 50). Furthermore, we analyzed the effect of H_2O_2 and BSO on modifying members of the TIMP family, mainly TIMP-1 and TIMP-3, that have been shown to play a pivotal role as endogenous regulators of MMPs (14, 18). TIMP-1 mRNA expression was significantly lowered by ~70–75% (Fig. 4*A*), and its protein was also significantly reduced by approximately two- to fourfold in response to oxidative stress (Fig. 4*B*). Similarly, TIMP-3 was reduced at mRNA and protein levels.

The stimulatory effect of oxidative stress on MMP expression and activity is mediated by HDAC. It has been shown that oxidative stress alters epigenetic mechanisms such as histone acetylation (41). Accordingly, we sought to test the contribution of HDAC on our proposed mechanism of oxidative stress-mediated induction of MMP activity and attenuation of the endothelial glycocalyx. Our data showed that H_2O_2 induced a fourfold increase in HDAC activity relative to control, an effect that was abrogated by TSA, a validated inhibitor of HDAC enzyme activity (Fig. 4*C*) (46). Furthermore, HDAC inhibition normalized MMP activity in H_2O_2-treated cells (Fig. 4, *D* and *E*). When combined with H_2O_2, TSA was capable of increasing TIMP-1 and TIMP-3 mRNA expression by approximately three- and fourfold, and their protein levels by approximately threefold and 50%, respectively, compared with H_2O_2 alone (Fig. 5, *A* and *C*). In addition to its ability to restore levels of TIMPs, TSA significantly inhibited H_2O_2-mediated increases in mRNA and protein levels of MMP-1, MMP-2, and MMP-9 ($P < 0.05$; Fig. 5, *A* and *B*). It is worth mentioning that TSA alone increased mRNA levels of TIMP-1 and TIMP-3 by 50% and 60% above basal levels, respectively (data not shown), which indicates that the basal level of HDAC activity is responsible for regulating the expression of TIMPs and MMPs. We further examined MMP and TIMP protein expression in response to another HDAC inhibitor, SAHA. Incubation with SAHA abrogated H_2O_2 effects on increasing MMPs and reducing their inhibitors, TIMPs, in endothelial cells (Fig. 5*D*).

Pharmacological inhibition of MMPs and HDAC reversed oxidative stress-induced shedding of syndecan-1. To test the hypothesis that shedding of syndecan-1 protein from the endothelial cell surface is secondary to the increased level of MMP and HDAC activity, we measured syndecan-1 protein in cell lysates and cell culture media in cells treated with H_2O_2 with and without marimastat and TSA. Our results showed that marimastat increased cellular syndecan-1 levels (H_2O_2: 0.9 ± 0.1 and H_2O_2 + marimastat: 2.3 ± 0.2, $P < 0.001$) and reduced its shedding from the endothelial cell surface (H_2O_2: 18.6 ± 0.8 and H_2O_2 + marimastat: 7.6 ± 0.5, $P < 0.001$; Fig. 6, *A* and *B*). Similarly, HDAC inhibition, via TSA, increased syndecan-1 in cell lysates by 2.5-fold and reduced its appearance in cell culture media by ~40% (Fig. 6, *A* and *B*). We further examined this hypothesis using SAHA, which inhibits HDAC class I, II, and IV, and SB-3CT, a selective inhibitor for MMP-2 and MMP-9. Incubation with SAHA and SB-3CT increased syndecan-1 protein in endothelial cell lysates by 72% and 46%, respectively ($P < 0.05$; Fig. 6*C*).

Marimastat and TSA protect against endothelial glycocalyx degradation and SOD3 loss. We showed above that marimastat and TSA interfered with the loss of syndecan-1 from the endothelial surface under conditions of oxidative stress. Thus, we sought to investigate the effect of marimastat and TSA on protecting the structure of the endothelial glycocayx. To this end, HAMECs were treated with H_2O_2 with and without the broad-spectrum MMP inhibitor marimastat, the specific MMP-2/MMP-9 inhibitor SB-3CT (29), and the broad-spectrum HDAC inhibitors TSA and SAHA (61) for 4 h and then stained with WGA to label cell surface HS-GAGs. MMP and HDAC inhibitors maintained the expression of HS-GAGs and prevented H_2O_2- mediated attenuation of the endothelial glycocalyx (Fig. 7*A*). The fluorescence intensity of WGA staining increased by 94%, 70%, 117%, and 65% when cells under oxidative stress were treated with marimastat, TSA, SAHA, and SB-3CT, respectively ($P < 0.01$; Fig. 7*B*).

Endothelial glycocalyx tethers and concentrates SOD3, which protects the endothelium against oxidative stress (16, 58). We expect that degradation of the endothelial glycocalyx results in an accelerated loss of GAG-attached SOD3. Therefore, we sought to test SOD3 expression and shedding in response to oxidative stress. Coinciding with the loss of syndecan-1 that was described above, we found a similar pattern of shedding of SOD3. This was detected by Western blot analysis of cell lysates and immunoprecipitated cell media after the induction of oxidative stress. Protein levels of SOD3 decreased significantly (50%) in HAMECs after 4 h of induced oxidative stress (Fig. 8*A*), whereas its levels in cell culture media increased by severalfold (Fig. 8*C*), indicating shedding of SOD3 from the cell surface into a soluble form. Pharmacological inhibition of MMPs, via marimastat, increased cellular levels of SOD3 protein by ~45% when combined with oxidative stress-inducing agents (Fig. 8*A*) and reduced SOD3 in cell culture media by severalfold (Fig. 8*C*). Likewise, HDAC inhibition increased SOD3 levels in cellular lysates (H_2O_2: 2.1 ± 0.1 and H_2O_2 + TSA: 1.7 ± 0.2, $P < 0.05$; Fig. 8*A*) and reduced them in cell culture media (H_2O_2: 2.8 ± 0.2 and H_2O_2 +

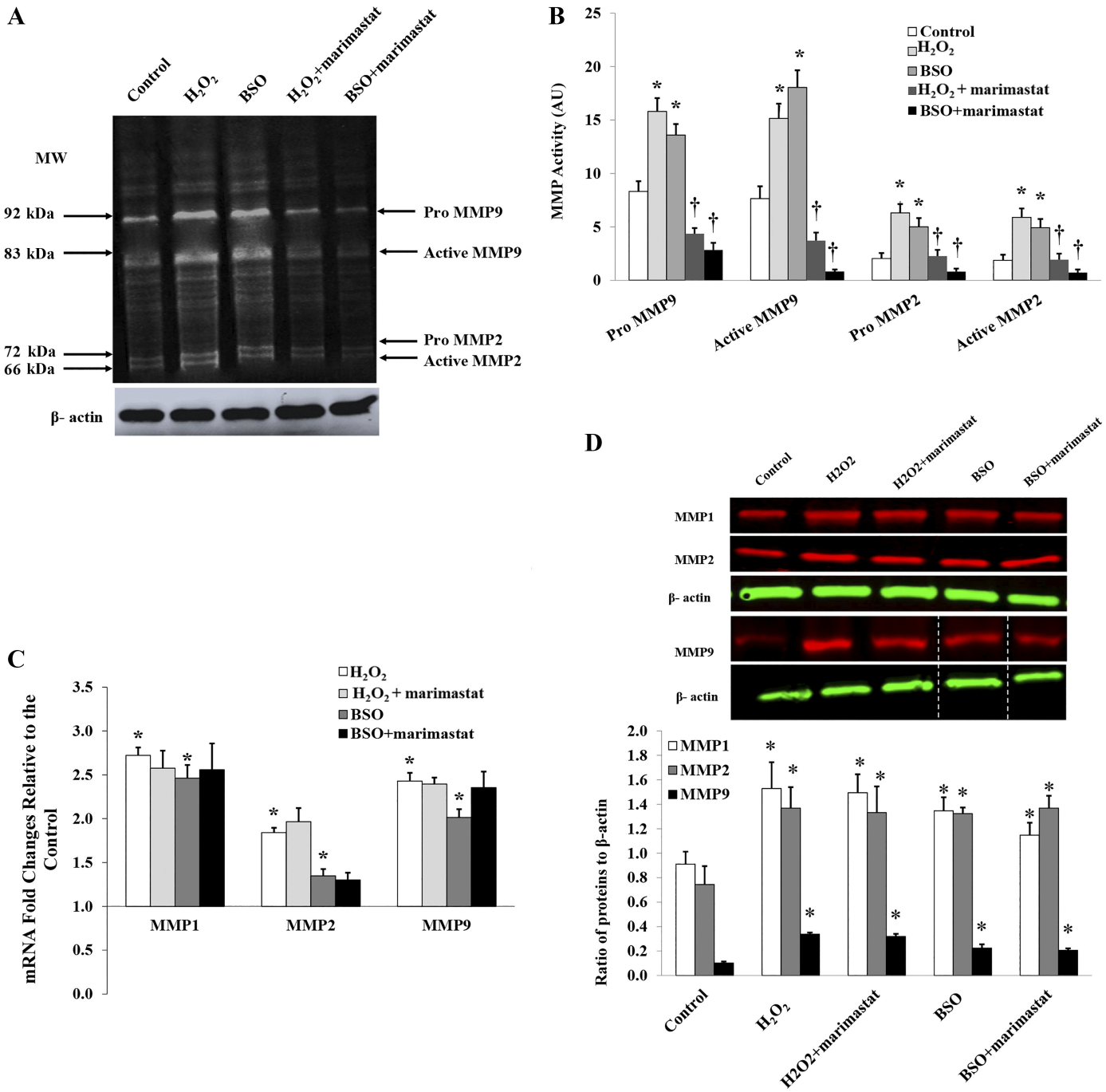

Fig. 3. Matrix metalloproteinase (MMP) activity in response to oxidative stress in human adipose microvascular endothelial cells (HAMECs). *A*: MMP-9 and MMP-2 activity in gelatin zymography of conditioned culture media collected from untreated cells (control) or cells treated with H_2O_2 (2×10^{-4} mol/l) or buthionine sulfoximine (BSO; 10^{-3} mol/l) with or without marimastat (50 μmol/l) for 4 h . *B*: β-actin was used as an internal control. *C*: densitometric analysis of MMP zymography bands. Results represent the mean log of 3 independent experiments. mRNA levels of MMP-1, MMP-2, and MMP-9 were measured by real-time PCR in cells treated with H_2O_2 or BSO with or without marimastat. Results represent fold changes relative to the untreated control. *D*: Western blot analysis and signal relative intensity quantification of MMP-1, MMP-2, and MMP-9 protein expression in HAMECs. *$P < 0.05$ for comparisons with control; †$P < 0.05$ for comparisons with H_2O_2 or BSO. All results represent means ± SD of 3 independent experiments (triplicates for each group for each experiment). The white dashed line indicates areas where gels were spliced for labeling purposes.

TSA: 0.6 ± 0.3, $P < 0.001$; Fig. 8*C*). Incubation with SAHA and SB-3CT increased SOD3 protein in endothelial cell lysates by 70% and 63%, respectively ($P < 0.001$; Fig. 8*B*). Collectively, these data led to the conclusion that HDAC and MMPs play an important role in mediating oxidative stress-induced modulation of the endothelial glycocalyx and loss of essential cellular protein associated with the endothelial glycocalyx such as syndecan-1 and SOD3.

Oxidative stress induced alterations in biomechanical properties in HAMECs. After confirming the link between oxidative stress and glycocalyx degradation, we sought to explore the effect of oxidative stress induced glycocalyx degradation on

endothelial cell biomechanics, which is dependent on the cellular glycocalyx and cytoskeletal structure (43). To investigate oxidative stress-induced changes in the elasticity of HAMECs, we used the AFM indentation technique (Fig. 9*A*). This technique was used to record the elastic modulus (Fig. 9*B*) in HAMECs before and after treatment with H_2O_2. The average elastic modulus of HAMECs treated with H_2O_2 (2.46 ± 0.2 kPa) was 2.5 times higher than control (0.985 ± 0.08

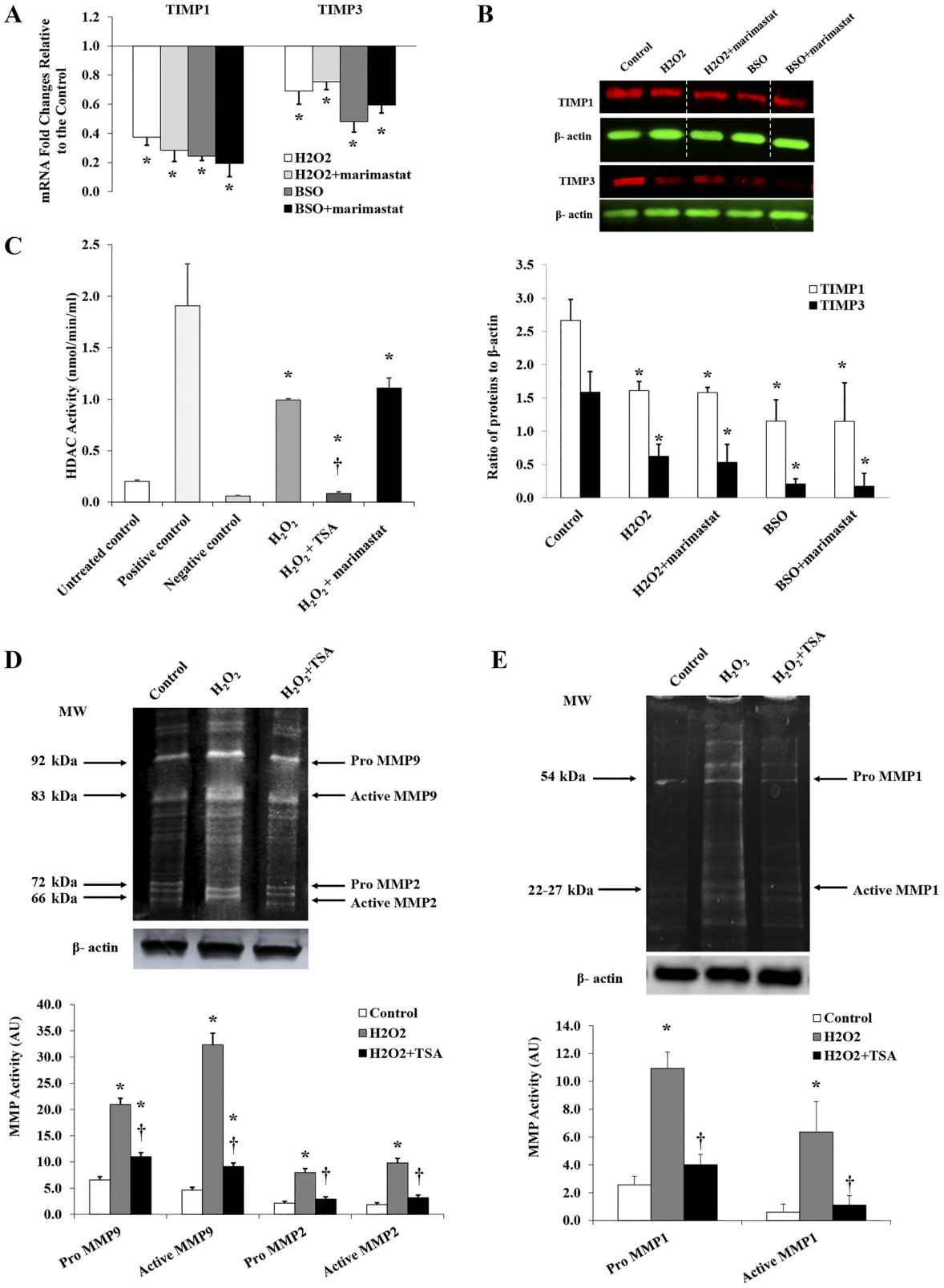

kPa). Marimastat and TSA restored the elasticity of HAMECs to levels that were close to control; the elastic modulus measured by AFM decreased by 43% and 55% after the addition of marimastat and TSA, respectively (Fig. 9*C*).

DISCUSSION

The principal findings of this study were that *1*) oxidative stress induced rarefaction and degradation of the microvascular endothelial glycocalyx and increased stiffness of endothelial cells as measured by AFM; *2*) MMPs are the principal cellular proteases involved in oxidative stress-induced degradation of the endothelial glycocalyx; *3*) direct inhibition of MMPs impeded oxidative stress-induced shedding of HSPGs from the endothelial cell surface and maintained the integrity of the endothelial glycocalyx; and *4*) oxidative stress augmented HDAC activity, a mechanism that might regulate the expression and activity of MMPs and TIMPs in endothelial cells. Figure 10 shows the main hypothesis and major findings.

Our results demonstrated that the endothelial glycocalyx exhibits a reaction to oxidative stress that is characterized by notable loss of HSPGs by means of shedding from the endothelial cell surface into the cell culture medium. Syndecans, one of the major HSPG core proteins in endothelial cells to which GAGs bind, were significantly lost from the endothelial cell surface. Apparently, the degradation of endothelial surface GAGs and HSPGs is faster than the endothelial cell potential to compensate. This is evident from our results showing that despite a significant increase in mRNA levels of syndecan-1, syndecan-2, and syndecan-3 isoforms, protein levels of syndecan-1, syndecan-2, and syndecan-3 from HAMECs treated with H_2O_2 or BSO was still lower than control. This indicates that under conditions of oxidative stress, cell surface proteoglycan degradation surpasses the capacity of cellular repair and homeostatic mechanisms. Therefore, interventions that inhibit glycocalyx-degrading enzymes or enhance glycocalyx repair are required to avert oxidative stress-induced endothelial dysfunction.

Our results agree with the study by Singh et al. (49) demonstrating that H_2O_2 treatment of glomerular endothelial cells, a renal microvascular endothelial cell line, induced GAG loss from the endothelial surface rather than reducing GAG synthesis. The clinical significance of these findings originates from a previous report demonstrating that the loss of the negatively charged GAG layer and its lodged albumin culminates into edema and microalbuminuria in a myriad of pathological conditions (45). This phenomenon has been reported in the myocardium after myocardial infarction, in coronary arteries after reperfusion, and in renal glomeruli after endotoxemia and glomerulonephritis (35, 40). Lipowsky et. al. (30, 31) reported a similar phenomenon of glycan shedding and glycocalyx attenuation in murine mesenteric microvessels in response to inflammatory agents and oxidative stress.

Also, we found that the increased stiffness of HAMECs after exposure to oxidative stress can be attributed, at least partially, to loss of the glycocalyx, even though we did not rule out the role of cytoskeletal changes after exposure to oxidative stress.

Our findings highlight MMPs as a major contributor to oxidative stress-induced loss of the glycocalyx from the vascular endothelium. Induction of oxidative stress resulted in a significant upregulation of MMP expression and activity. On the other hand, inhibitors of MMPs, TIMP-1 and TIMP-2, were downregulated. This link between MMP upregulation and glycocalyx density was confirmed using marimastat, a direct and broad-spectum MMP inhibitor, to antagonize the effect of MMPs on the HSPG component of the glycocalyx. Our results showed that marimastat prevented shedding of syndecan-1 from the cell membrane of HAMECs after H_2O_2 and BSO treatment in endothelial cells and subsequently maintained the density of GAGs. Furthermore, marimastat restored endothelial cell elasticity and corrected or reversed the stiffness that was observed in HAMECs after treatment with H_2O_2 (Fig. 9). These results were confirmed using the specific MMP-2/MMP-9 inhibitor SB-3CT, which reversed the loss of syndecan-1 and the endothelial glycocalyx from HAMECs treated with H_2O_2. A role of MMPs has also been suggested in previous studies that demonstrated restoration of the endothelial glycocalyx through modulation of MMP activity (62, 63). Collectively, these findings provide a mechanistic interpretation for the MMP role in vascular dysfunction involving oxidative stress in CVD and other conditions such as metabolic syndrome, diabetes, atherosclerosis, and myocardial ischemia, where high oxidative stress is a common factor in the pathogenesis and disease progression (1).

It is important to emphasize that the consequences of degradation of the glycocalyx are not limited to the loss of the endothelial lining but extend to loss of functional molecules harbored in the glycocalyx. One of the most important of these molecules is SOD3. A few reports have asserted that SOD3 is exclusively expressed in vascular smooth muscle cells and then translocates to get lodged onto HS-GAGs on the vascular endothelial cell membrane (16, 24, 36). Nevertheless, we found considerable basal expression of SOD3 in HAMECs that was significantly reduced after the induction of oxidative stress. Moreover, the increased levels of SOD3 protein in the cell culture medium in response to oxidative stress indicates that degradation of the endothelial glycocalyx is accompanied by a

Fig. 4. Tissue inhibitor of metalloproteinase (TIMP)-1 and TIMP-3 mRNA and protein expression levels in human adipose microvascular endothelial cells (HAMECs) under oxidative stress. Cells were treated with H_2O_2 (2×10^{-4} mol/l) or buthionine sulfoximine (BSO; 10^{-3} mol/l) with or without marimastat (50 μmol/l) for 4 h. *A*: TIMP-1 and TIMP-3 mRNA levels measured by real-time PCR. *B*: Western blot analysis and signal relative intensity quantification of TIMP-1 and TIMP-3 protein expression in HAMECs. Results of mRNA expression represent fold changes relative to the untreated control from 3 independent experiments. *C*: cells were treated with H_2O_2 (2×10^{-4} mol/l) with or without marimastat (50 μmol/l) or trichostatin (TSA; 1 μmol/l) for 4 h. Histone deacetylase (HDAC) activity was measured using HDAC Activity Assay Kit as described in MATERIALS AND METHODS. Untreated cells, TSA-treated cells, and human recombinant HDAC1-treated cells were used as an untreated control, a negative control, and a positive control, respectively. *D* and *E*: matrix metalloproteinase (MMP)-9 and MMP-2 activity in gelatin zymography (*D*) and MMP-1 activity in collagen zymography (*E*) of conditioned culture media collected from untreated cells (control) or cells treated with H_2O_2 and H_2O_2 + TSA. β-Actin was used as an internal control. Charts represent the densitometric analysis of MMP zymography bands. AU, arbitrary units. All results represent means ± SD of 3 independent experiments (triplicates for each group in each experiment). $*P < 0.05$ for comparisons with the control groups; $\dagger P < 0.05$ for comparisons with H_2O_2- or BSO-treated groups. The white dashed line indicates areas where gels were spliced for labeling purposes.

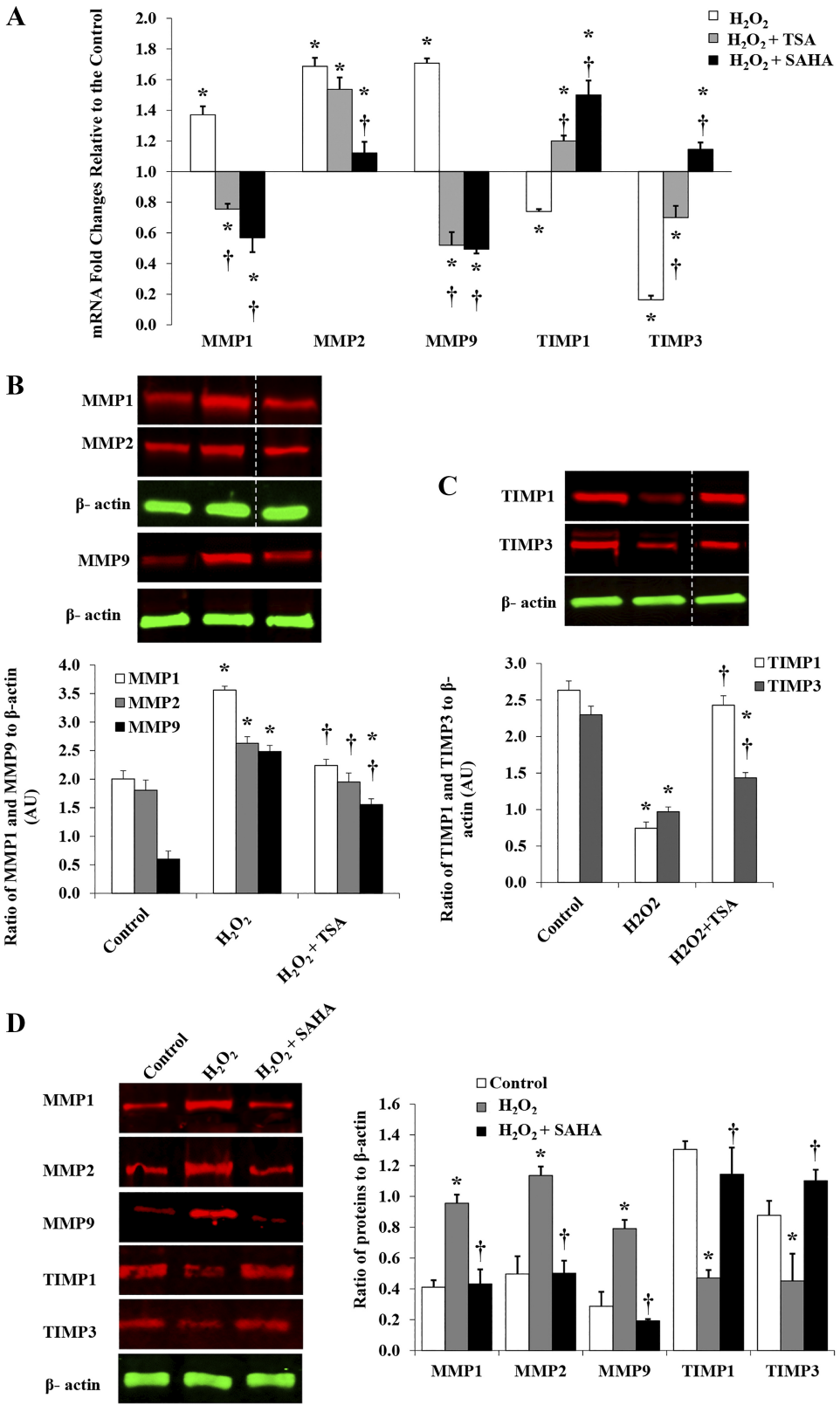

Fig. 5. Effects of inhibition of histone deacetylase (HDAC) activity on mRNA and protein expression of matrix metalloproteinases (MMPs) and tissue inhibitors of metalloproteinase (TIMPs). Cells were treated with H_2O_2 (2×10^{-4} mol/l) with or without marimastat (50 μmol/l), trichostatin (TSA; 1 μmol/l), or suberoylanilide hydroxamic acid (SAHA; 5 μmol/l) for 4 h. *A*: mRNA levels of MMP-1, MMP-2, MMP-9, TIMP-1, and TIMP-3 in human adipose microvascular endothelial cells (HAMECs) measured by real-time PCR. Results of mRNA expression represent fold changes relative to the untreated control from 3 independent experiments. *B–D*: Western blot analysis and signal relative intensity quantification of MMP-1, MMP-2, MMP-9, TIMP-1, and TIMP-3 protein expression in HAMECs. Results of protein expression represent means ± SD of 3 independent experiments (triplicates for each group in each experiment). *$P < 0.05$ for comparisons with the control groups; †$P < 0.05$ for comparisons with H_2O_2. The white dashed line indicates areas where gels were spliced for labeling purposes.

loss of proteins that are critical to cell integrity such as SOD3. Interestingly, pharmacological inhibition of MMPs via marimastat salvaged SOD3 protein by interfering with HSPG shedding from the endothelial cell surface.

To this point, our results indicated a notable involvement of a genetic regulatory mechanism in the endothelial response to oxidative stress that was evident by significant and consistent changes in mRNA levels of MMPs and TIMPs. Given the

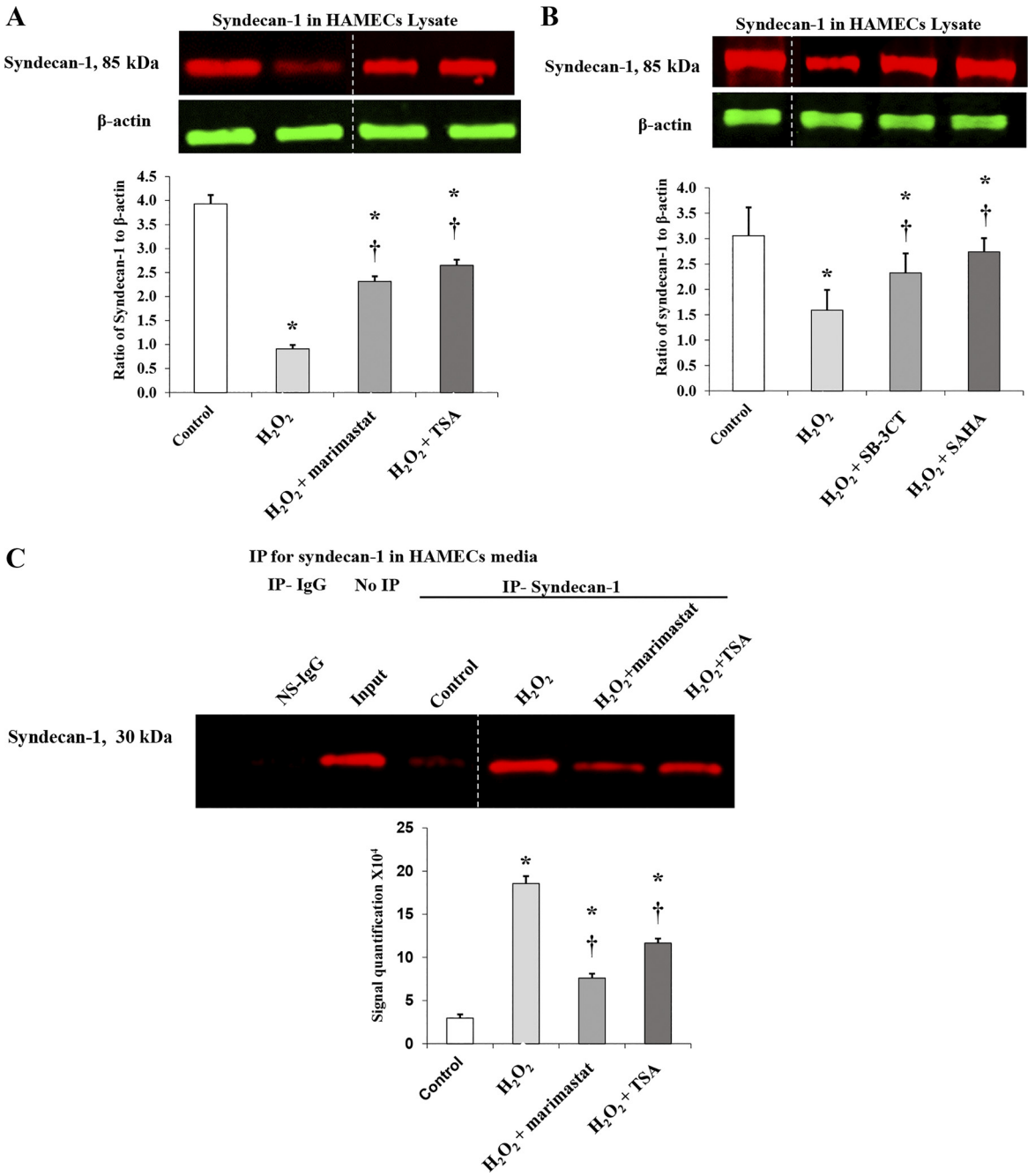

Fig. 6. Effects of matrix metalloproteinases (MMPs) and histone deacetylase (HDAC) inhibition on syndecan-1 shedding. *A*: cells were treated with H_2O_2 (2×10^{-4} mol/l) with or without marimastat (50 μmol/l) or trichostatin (TSA; 1 μmol/l) for 4 h. *B*: in another set of experiments, cells were treated with H_2O_2 (2×10^{-4} mol/l) with or without suberoylanilide hydroxamic acid (SAHA; 5 μmol/l) or 2-[(4-phenoxyphenylsulfonyl)methyl]thiirane (SB-3CT; 100 nmol/l) for 4 h. Western blot analysis and signal relative intensity quantification of syndecan-1 and extracellular superoxide dismutase (SOD3) protein expression in human adipose microvascular endothelial cells (HAMECs) are shown. β-Actin was used as a loading control for both proteins that were measured in the same gel (SOD3 data are shown in Fig. 8*B*). *C*: Western blot analysis of cleaved syndecan-1 in HAMEC culture media. Conditioned media were immunoprecipitated (IP) with syndecan-1 antibody or rabbit IgG as a control for nonspecific IgG (NS-IgG) and immunoblotted for syndecan-1. Media of untreated cells were used as a negative control, and media before IP were used to demonstrate that protein bands correspond to the expected molecular weight. Results represent means ± SD of 3 independent experiments (triplicates for each group in each experiment). *$P < 0.05$ for comparisons with control; †$P < 0.05$ for comparisons with H_2O_2. The white dashed line indicates areas where gels were spliced for labeling purposes.

volume of literature reporting epigenetic regulation of cardiovascular biology in health and disease, we sought to further explore the involvement of epigenetic regulation of the endothelial response to oxidative stress. HDACs play essential roles in many cardiovascular biological processes spanning transcriptional and translational regulation (60). Interestingly, we found that HDAC activity was upregulated in response to oxidative stress and that inhibition of HDAC activity, via TSA or SAHA, normalized MMP expression and restored basal levels of TIMP-1 and TIMP-3. These

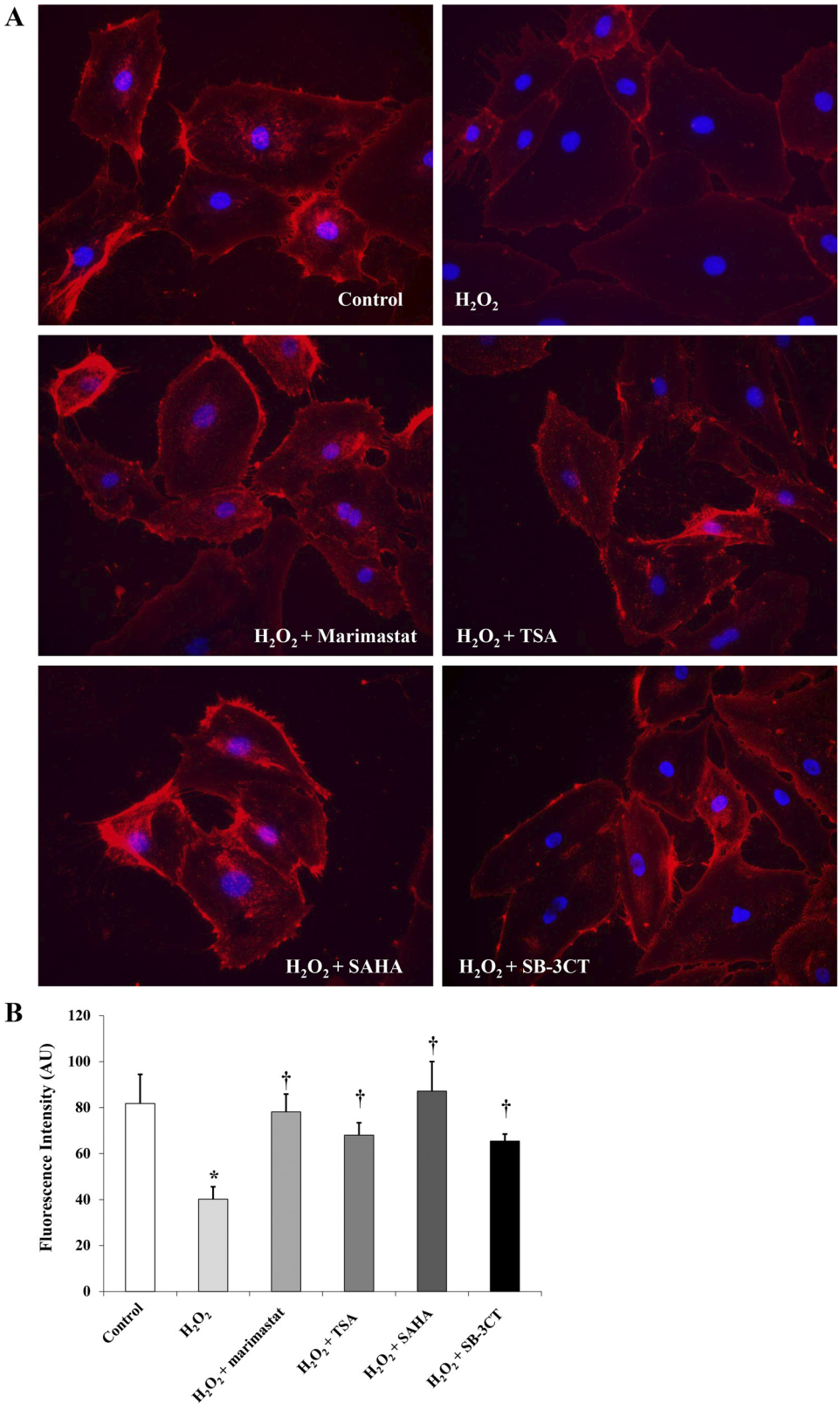

Fig. 7. Effects of matrix metalloproteinases (MMPs) and histone deacetylase (HDAC) inhibition on glycocalyx integrity. Human adipose microvascular endothelial cells (HAMECs) were treated with control vehicle, H_2O_2 (2×10^{-4} mol/l), H_2O_2 + marimastat (50 μmol/l), H_2O_2 + trichostatin (TSA; 1 μmol/l), H_2O_2 + suberoylanilide hydroxamic acid (SAHA; 5 μmol/l), or H_2O_2 + SB-3CT (100 nmol/l) for 4 h. *A*: cells were stained with fluorescent wheat germ agglutinin (WGA) and imaged using a fluorescent microscope. *B*: the fluorescent signal was then quantified by ImageJ software. Shown is a graphic presentation of the means of 3 independent experiments ± SD (triplicates for each group in each experiment). AU, arbitrary units. *$P < 0.05$ for comparisons with control; †$P < 0.05$ for comparisons with H_2O_2.

findings verified the role of HDAC in mediating oxidative stress-induced upregulation of MMPs in endothelial cells and consequently endothelial glycocalyx attenuation. Furthermore, our results provide mechanistic insights into the role of HDAC activity in a myriad of conditions including cardiovascular and pulmonary disease conditions (8, 38, 51). To our knowledge, our study is the first to investigate the interplay between HDAC-mediated epigenetic regula-

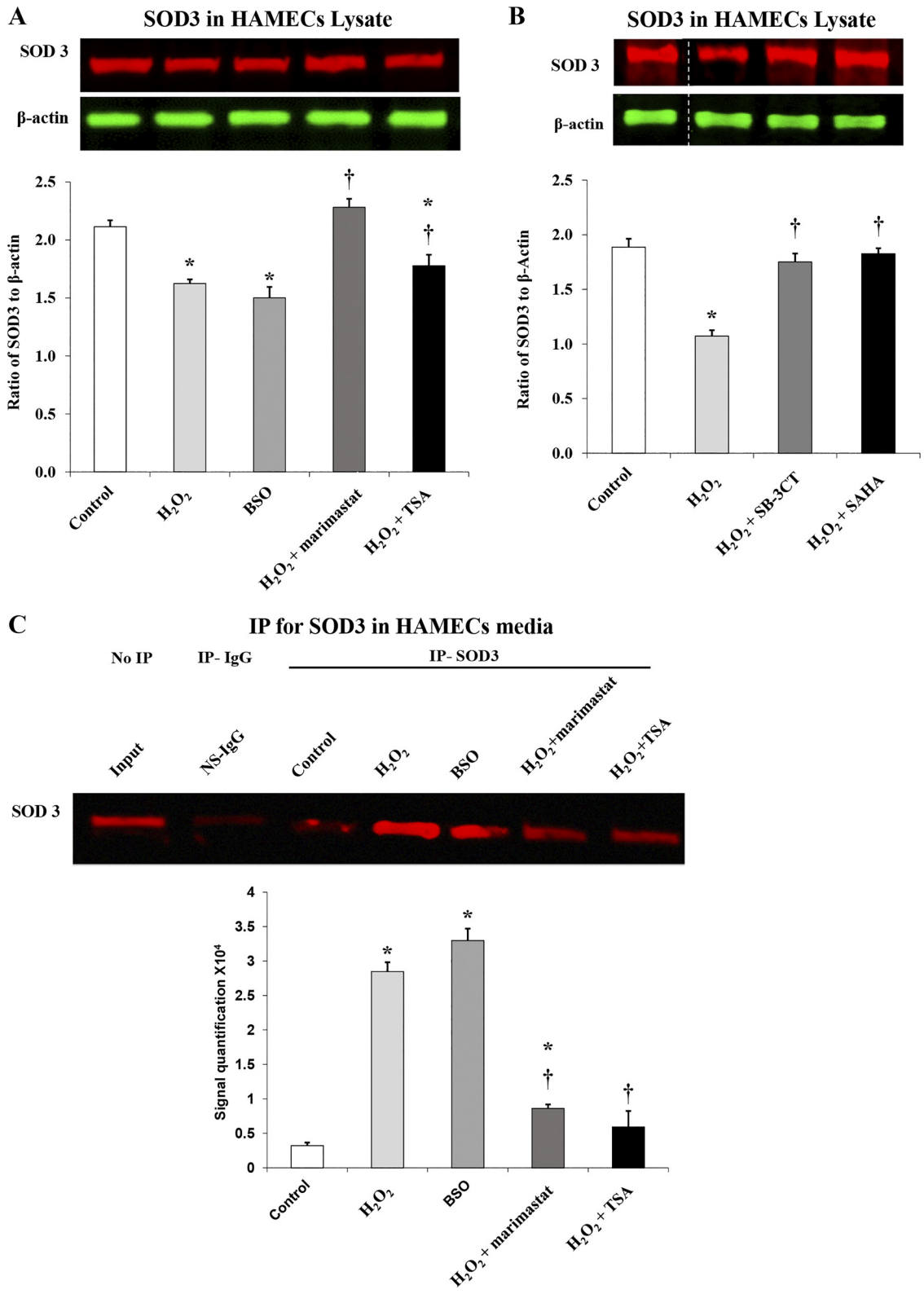

Fig. 8. Effects of matrix metalloproteinases (MMPs) and histone deacetylase (HDAC) inhibition on extracellular superoxide dismutase (SOD3) shedding. *A*: cells were treated with H_2O_2 (2×10^{-4} mol/l) or BSO (10^{-3} mol/l) with or without marimastat (50 μmol/l) or trichostatin (TSA; 1 μmol/l) for 4 h. *B*: in another set of experiments, cells were treated with H_2O_2 (2×10^{-4} mol/l) with or without suberoylanilide hydroxamic acid (SAHA; 5 μmol/l) or SB-3CT (100 nmol/l) for 4 h. *A* and *B*: Western blot analysis and signal relative intensity quantification of SOD3 protein expression in HAMECs. *C*: Western blot analysis of cleaved SOD3 in human adipose microvascular endothelial cell (HAMEC) culture media. Conditioned media were immunoprecipitated (IP) with SOD3 antibody or mouse IgG as a control for nonspecific IgG (NS-IgG) and immunoblotted for SOD3. Media of untreated cells were used as a negative control, and media before IP were used to demonstrate that protein bands correspond to the expected molecular weight. Results represent means ± SD of 3 independent experiments (triplicates for each group in each experiment). *$P < 0.05$ for comparisons with control; †$P < 0.05$ for comparisons with H_2O_2. The white dashed line indicates areas where gels were spliced for labeling purposes.

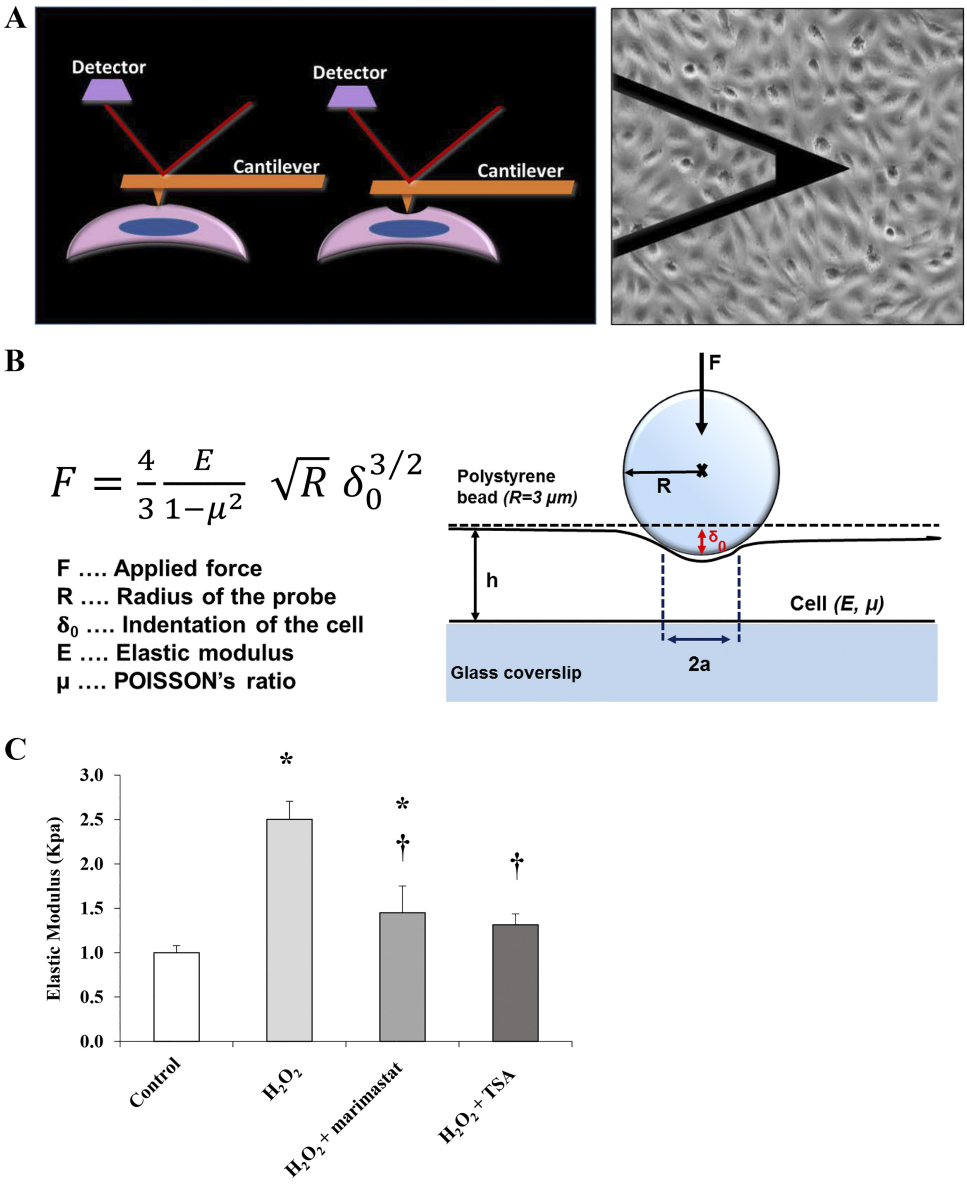

Fig. 9. Effects of oxidative stress on endothelial cell elasticity. *A*, *left*: illustration of the principle of atomic force microscope (AFM) in which the tip of the cantilever deflects along the vertical axis according to the mechanical properties of the underlying surface. *A*, *right*: the bright-field microscope showing the tip of a scanning AFM probing the biomechanical properties of a confluent human adipose microvascular endothelial cell (HAMEC) cell culture. *B*: derivation of the Hertzian model to calculate force and elastic modulus of a surface probed by the AFM tip. *C*: effects of H_2O_2 with and without marimastat or trichostatin A (TSA) on HAMEC elasticity. Results represent means ± SD of 3 independent experiments (triplicates for each group in each experiment). *$P < 0.05$ for comparison of H_2O_2-treated cells with the control group; †$P < 0.05$ for comparison of groups treated with H_2O_2 + marimastat or H_2O_2 + TSA with those treated with H_2O_2 only.

tion of oxidative stress response genes and structural and functional changes at the endothelial cell level.

The exact mechanism by which HDAC regulate MMP expression and activity is not clear. Our data suggest that this effect is partially mediated via reducing TIMPs, the endogenous MMP inhibitors. However, a direct stimulatory effect of HDAC on MMP expression was evident by TSA-mediated reductions in MMP expression, a finding that is contradictory to the predominant view of HDAC transcriptional repression activity. Although the major function of HDAC is to suppress gene transcription through histone deacetylation, this effect is gene dependent, and a paradoxical induction of gene transcription has been reported by others (21, 32). In agreement with our findings, previous studies have shown that HDAC hyperactivity contributes to ECM remodeling in mouse models via increasing MMP-2 and MMP-9 expression (34). Furthermore, other studies have demonstrated reductions in MMP-2 and MMP-9 levels in cancer in response to TSA treatment (9, 57). In the present study, HDAC inhibition also restored the expression of TIMPs, intrinsic MMP inhibitors. This is also in agreement with other studies that reported restoration of another MMP regulator, RECK, after HDAC inhibition (21, 28). These studies and ours highlight the diversity of HDAC function, which is often gene dependent.

Thus, it is clear that the simplistic overview of the role of HDAC in transcriptional activity as a mere repressor does not explain the transcriptional profile in which mRNA transcripts of some genes increase, whereas that of other genes decrease, in the microvascular endothelium. There must be a higher order of interaction between the products of gene transcription and translation, and this higher order of interaction might involve other epigenetic regulatory mechanisms including DNA methylation or microRNA (48). It might also encompass an effect of HDAC on nonhistone proteins that is mechanistically different than its effect on histone proteins (13). Thus, further investigations to dissect transcriptional stimulatory versus inhibitory mechanisms of HDAC in the context of oxidative stress and MMP pathways in the endothelium are required.

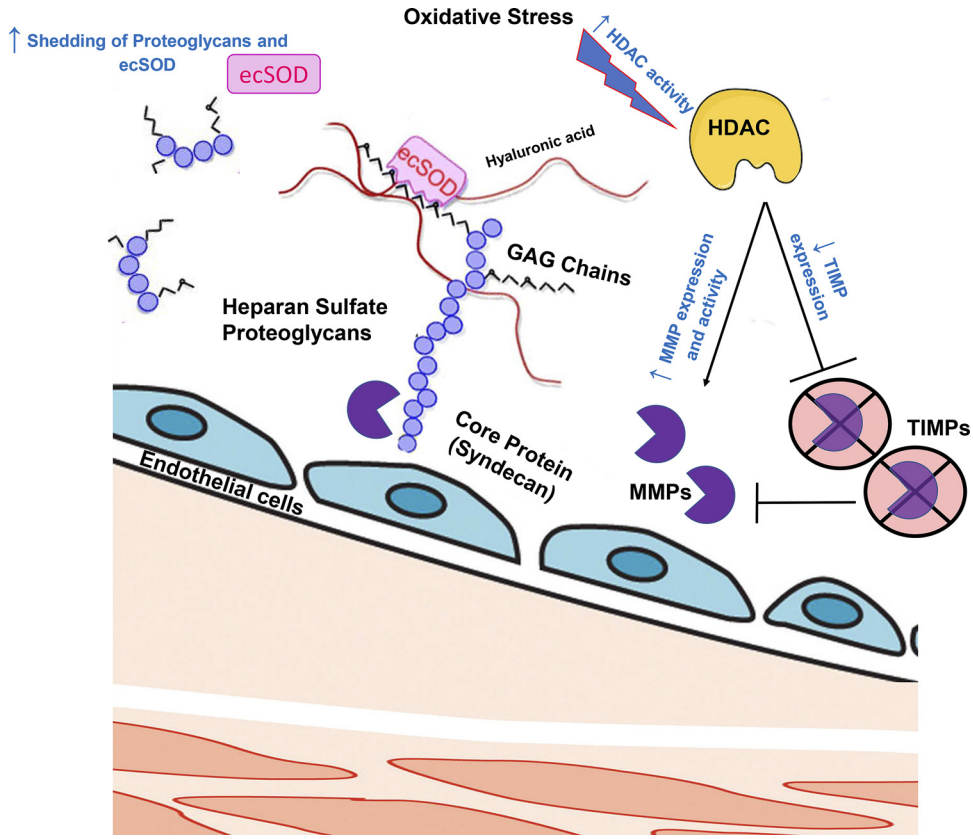

Fig. 10. Hypothetical schematic of the role of histone deacetylase (HDAC) and matrix metalloproteinases (MMPs) in mediating oxidative stress-induced disruptions in the endothelial glycocalyx. Oxidative stress attenuates endothelial glycocalyx density via decreasing the cell surface content of glycosaminoglycans (GAGs) and heparan sulfate proteoglycans (HSPGs). An epigenetic regulatory mechanism that involves HDAC mediates the oxidative stress-induced upregulation of MMPs and downregulation of tissue inhibitors of metalloproteinase (TIMPs). The induced MMP expression and activity results in increased shedding of syndecans and the associated GAGs and extracellular superoxide dismutase (ecSOD).

Our data also indicate a role for HDAC in endothelial glycocalyx degradation under conditions of oxidative stress. In support of this assumption, we demonstrated that inhibition of HDAC activity via TSA or SAHA reduced shedding of syndecan-1 and SOD3 and maintained endothelial cell surface GAGs. Furthermore, HDAC inhibition reversed the endothelial stiffness that was induced by oxidative stress. Collectively, these observations highlight the role of HDAC in oxidative stress-induced modulation in MMP expression and the subsequent alterations in endothelial glycocalyx structure and function.

Limitations. It is noteworthy that the use of HAMECs as the cell model of choice was well suited for the objectives and aims of the present study since this primary cell line is isolated from human visceral adipose tissue and is well representative of the systemic resistance arterioles that are known to contain the bulk of the glycocalyx (2). Also, HAMECs exhibited a high basal expression of SOD3, unlike macrovascular endothelial cells, including human umbilical vascular endothelial cells, one of the most frequently used macrovascular cells, that do not express SOD3 (16, 24, 36). Furthermore, while oxidative stress manifests in macrovascular structures as endothelial activation, inflammatory cell infiltration, and smooth muscle proliferation and migration, in the microvasculature, endothelial dysfunction manifests as loss of the glycocalyx and rarefaction. Nevertheless, it is worth noting that the cell culture model that we used is not without limitations. For example, unlike in vivo models of inflammation and endothelial dysfunction, our model lacks the inflammatory cells and intercellular interactions that are found in animal models or ex vivo-isolated vessels. Regarding the AFM measurements to assess the change in elasticity of HAMECs before or after oxidative stress, it is worth noting that AFM measurements are an average of the vertical force measured at the point of indentation on the cell surface. Our results demonstrate the elastic modulus registered at 500-nm indentation depth, which, according to the two-layer model reported by Marsh and Waugh (37), involves the cell body. Accordingly, we cannot rule out the biomechanical contribution of cytoskeletal modulation to the increased elastic modulus observed in HAMECs under conditions of oxidative stress. Furthermore, we should acknowledge the heterogeneity in reporting glycocalyx elastic modulus among different studies (37, 43, 55). This heterogeneity could be caused by factors related to endothelial cell type, cell culture conditions, or AFM method specifics such as probe bead diameter and indentation depth.

Summary and conclusions. In summary, the present study demonstrates the role of oxidative stress in reducing endothelial glycocalyx density and decreasing the cell surface content of HSPGs and SOD3. Our study also refers to HDAC as a novel epigenetic regulatory mechanism that mediates the oxidative stress-induced upregulation of MMPs and downregulation of TIMPs. These findings highlight a novel therapeutic end point and its associated therapeutic target. The therapeutic end point is the integrity of microvascular endothelial glycocalyx density and composition including its content of syndecan-1 and SOD3. The target is the activity of MMP and HDAC enzymes mediating the loss of the glycocalyx under oxidative stress conditions and the balance between MMP activity and their inhibitors (TIMPs). It is worth mentioning that some of these inhibitors are currently under trials for their mitigating effect in CVDs and pulmonary diseases (7, 33). Therefore, a

potent and selective inhibitor of MMPs or HDACs may be an important potential therapeutic target for ameliorating the detrimental effect of oxidative stress on the microvascular endothelial glycocalyx and the negative effects of CVD on tissue perfusion.

GRANTS

This work was supported by the following funding sources: National Heart, Lung, and Blood Institute Grants R01-HL-095701 (to S. A. Phillips) and 1-K99-HL-140049-01 (to A. M. Mahmoud) and American Heart Association Grant 15POST24480172 (to A. M. Mahmoud).

DISCLOSURES

No conflicts of interest, financial or otherwise, are declared by the authors.

AUTHOR CONTRIBUTIONS

M.A., A.M.M., and S.A.P. conceived and designed research; M.A., A.M.M., and E.L.M. performed experiments; M.A. and A.M.M. analyzed data; M.A., A.M.M., and S.A.P. interpreted results of experiments; M.A. and A.M.M. prepared figures; M.A. and A.M.M. drafted manuscript; M.A., A.M.M., I.L., and S.A.P. edited and revised manuscript; M.A., A.M.M., E.L.M., I.L., and S.A.P. approved final version of manuscript.

REFERENCES

1. **Ali MA, Schulz R.** Activation of MMP-2 as a key event in oxidative stress injury to the heart. *Front Biosci (Landmark Ed)* 14: 699–716, 2009.
2. **Arkill KP, Knupp C, Michel CC, Neal CR, Qvortrup K, Rostgaard J, Squire JM.** Similar endothelial glycocalyx structures in microvessels from a range of mammalian tissues: evidence for a common filtering mechanism? *Biophys J* 101: 1046–1056, 2011. doi:10.1016/j.bpj.2011.07.036.
3. **Beaudeux JL, Giral P, Bruckert E, Foglietti MJ, Chapman MJ.** Matrix metalloproteinases, inflammation and atherosclerosis: therapeutic perspectives. *Clin Chem Lab Med* 42: 121–131, 2004. doi:10.1515/CCLM.2004.024.
4. **Becker BF, Jacob M, Leipert S, Salmon AH, Chappell D.** Degradation of the endothelial glycocalyx in clinical settings: searching for the sheddases. *Br J Clin Pharmacol* 80: 389–402, 2015. doi:10.1111/bcp.12629.
5. **Bielecka-Dabrowa A, von Haehling S, Aronow WS, Ahmed MI, Rysz J, Banach M.** Heart failure biomarkers in patients with dilated cardiomyopathy. *Int J Cardiol* 168: 2404–2410, 2013. doi:10.1016/j.ijcard.2013.01.157.
6. **Billings PC, Pacifici M.** Interactions of signaling proteins, growth factors and other proteins with heparan sulfate: mechanisms and mysteries. *Connect Tissue Res* 56: 272–280, 2015. doi:10.3109/03008207.2015.1045066.
7. **Cao DJ, Wang ZV, Battiprolu PK, Jiang N, Morales CR, Kong Y, Rothermel BA, Gillette TG, Hill JA.** Histone deacetylase (HDAC) inhibitors attenuate cardiac hypertrophy by suppressing autophagy. *Proc Natl Acad Sci USA* 108: 4123–4128, 2011. doi:10.1073/pnas.1015081108.
8. **Cardinale JP, Sriramula S, Pariaut R, Guggilam A, Mariappan N, Elks CM, Francis J.** HDAC inhibition attenuates inflammatory, hypertrophic, and hypertensive responses in spontaneously hypertensive rats. *Hypertension* 56: 437–444, 2010. doi:10.1161/HYPERTENSIONAHA.110.154567.
9. **Chen Z, Yang Y, Liu B, Wang B, Sun M, Zhang L, Chen B, You H, Zhou M.** Promotion of metastasis-associated gene expression in survived PANC-1 cells following trichostatin A treatment. *Anticancer Agents Med Chem* 15: 1317–1325, 2015. doi:10.2174/1871520615666150520093040.
10. **de Meijer VE, Sverdlov DY, Popov Y, Le HD, Meisel JA, Nosé V, Schuppan D, Puder M.** Broad-spectrum matrix metalloproteinase inhibition curbs inflammation and liver injury but aggravates experimental liver fibrosis in mice. *PLoS One* 5: e11256, 2010. doi:10.1371/journal.pone.0011256.
11. **Derosa G, D'Angelo A, Ciccarelli L, Piccinni MN, Pricolo F, Salvadeo S, Montagna L, Gravina A, Ferrari I, Galli S, Paniga S, Tinelli C, Cicero AF.** Matrix metalloproteinase-2, -9, and tissue inhibitor of metalloproteinase-1 in patients with hypertension. *Endothelium* 13: 227–231, 2006. doi:10.1080/10623320600780942.
12. **Endo K, Takino T, Miyamori H, Kinsen H, Yoshizaki T, Furukawa M, Sato H.** Cleavage of syndecan-1 by membrane type matrix metalloproteinase-1 stimulates cell migration. *J Biol Chem* 278: 40764–40770, 2003. doi:10.1074/jbc.M306736200.
13. **Eom GH, Kook H.** Posttranslational modifications of histone deacetylases: implications for cardiovascular diseases. *Pharmacol Ther* 143: 168–180, 2014. doi:10.1016/j.pharmthera.2014.02.012.
14. **Fedak PW, Moravec CS, McCarthy PM, Altamentova SM, Wong AP, Skrtic M, Verma S, Weisel RD, Li RK.** Altered expression of disintegrin metalloproteinases and their inhibitor in human dilated cardiomyopathy. *Circulation* 113: 238–245, 2006. doi:10.1161/CIRCULATIONAHA.105.571414.
15. **Florian JA, Kosky JR, Ainslie K, Pang Z, Dull RO, Tarbell JM.** Heparan sulfate proteoglycan is a mechanosensor on endothelial cells. *Circ Res* 93: e136–e142, 2003. doi:10.1161/01.RES.0000101744.47866.D5.
16. **Fukai T, Ushio-Fukai M.** Superoxide dismutases: role in redox signaling, vascular function, and diseases. *Antioxid Redox Signal* 15: 1583–1606, 2011. doi:10.1089/ars.2011.3999.
17. **Galis ZS, Khatri JJ.** Matrix metalloproteinases in vascular remodeling and atherogenesis: the good, the bad, and the ugly. *Circ Res* 90: 251–262, 2002. doi:10.1161/res.90.3.251.
18. **Haas TL.** Endothelial cell regulation of matrix metalloproteinases. *Can J Physiol Pharmacol* 83: 1–7, 2005. doi:10.1139/y04-120.
19. **Ito K, Hanazawa T, Tomita K, Barnes PJ, Adcock IM.** Oxidative stress reduces histone deacetylase 2 activity and enhances IL-8 gene expression: role of tyrosine nitration. *Biochem Biophys Res Commun* 315: 240–245, 2004. doi:10.1016/j.bbrc.2004.01.046.
20. **Jaroszyński AJ, Jaroszyńska A, Przywara S, Zaborowski T, Książek A, Dąbrowski W.** Syndecan-4 is an independent predictor of all-cause as well as cardiovascular mortality in hemodialysis patients. *PLoS One* 11: e0163532, 2016. doi:10.1371/journal.pone.0163532.
21. **Jeon HW, Lee YM.** Inhibition of histone deacetylase attenuates hypoxia-induced migration and invasion of cancer cells via the restoration of RECK expression. *Mol Cancer Ther* 9: 1361–1370, 2010. doi:10.1158/1535-7163.MCT-09-0717.
22. **Jones CB, Sane DC, Herrington DM.** Matrix metalloproteinases: a review of their structure and role in acute coronary syndrome. *Cardiovasc Res* 59: 812–823, 2003. doi:10.1016/S0008-6363(03)00516-9.
23. **Kadoglou NP, Daskalopoulou SS, Perrea D, Liapis CD.** Matrix metalloproteinases and diabetic vascular complications. *Angiology* 56: 173–189, 2005. doi:10.1177/000331970505600208.
24. **Karlsson K, Lindahl U, Marklund SL.** Binding of human extracellular superoxide dismutase C to sulphated glycosaminoglycans. *Biochem J* 256: 29–33, 1988. doi:10.1042/bj2560029.
25. **Kataoka H, Ushiyama A, Kawakami H, Akimoto Y, Matsubara S, Iijima T.** Fluorescent imaging of endothelial glycocalyx layer with wheat germ agglutinin using intravital microscopy. *Microsc Res Tech* 79: 31–37, 2016. doi:10.1002/jemt.22602.
26. **Kummrow A, Frankowski M, Bock N, Werner C, Dziekan T, Neukammer J.** Quantitative assessment of cell viability based on flow cytometry and microscopy. *Cytometry A* 83A: 197–204, 2013. doi:10.1002/cyto.a.22213.
27. **Laviades C, Varo N, Fernández J, Mayor G, Gil MJ, Monreal I, Díez J.** Abnormalities of the extracellular degradation of collagen type I in essential hypertension. *Circulation* 98: 535–540, 1998. doi:10.1161/01.CIR.98.6.535.
28. **Lee KJ, Lee KY, Lee YM.** Downregulation of a tumor suppressor RECK by hypoxia through recruitment of HDAC1 and HIF-1alpha to reverse HRE site in the promoter. *Biochim Biophys Acta* 1803: 608–616, 2010. doi:10.1016/j.bbamcr.2010.01.004.
29. **Lee M, Villegas-Estrada A, Celenza G, Boggess B, Toth M, Kreitinger G, Forbes C, Fridman R, Mobashery S, Chang M.** Metabolism of a highly selective gelatinase inhibitor generates active metabolite. *Chem Biol Drug Des* 70: 371–382, 2007. doi:10.1111/j.1747-0285.2007.00577.x.
30. **Lipowsky HH, Gao L, Lescanic A.** Shedding of the endothelial glycocalyx in arterioles, capillaries, and venules and its effect on capillary hemodynamics during inflammation. *Am J Physiol Heart Circ Physiol* 301: H2235–H2245, 2011. doi:10.1152/ajpheart.00803.2011.
31. **Lipowsky HH, Lescanic A.** The effect of doxycycline on shedding of the glycocalyx due to reactive oxygen species. *Microvasc Res* 90: 80–85, 2013. doi:10.1016/j.mvr.2013.07.004.
32. **Liu LT, Chang HC, Chiang LC, Hung WC.** Histone deacetylase inhibitor up-regulates RECK to inhibit MMP-2 activation and cancer cell invasion. *Cancer Res* 63: 3069–3072, 2003.

33. **Liu T, Song D, Dong J, Zhu P, Liu J, Liu W, Ma X, Zhao L, Ling S.** Current understanding of the pathophysiology of myocardial fibrosis and its quantitative assessment in heart failure. *Front Physiol* 8: 238, 2017. doi:10.3389/fphys.2017.00238.
34. **Mani SK, Kern CB, Kimbrough D, Addy B, Kasiganesan H, Rivers WT, Patel RK, Chou JC, Spinale FG, Mukherjee R, Menick DR.** Inhibition of class I histone deacetylase activity represses matrix metalloproteinase-2 and -9 expression and preserves LV function postmyocardial infarction. *Am J Physiol Heart Circ Physiol* 308: H1391–H1401, 2015. doi:10.1152/ajpheart.00390.2014.
35. **Marechal X, Favory R, Joulin O, Montaigne D, Hassoun S, Decoster B, Zerimech F, Neviere R.** Endothelial glycocalyx damage during endotoxemia coincides with microcirculatory dysfunction and vascular oxidative stress. *Shock* 29: 572–576, 2008. doi:10.1097/SHK.0b013e318157e926.
36. **Marklund SL.** Expression of extracellular superoxide dismutase by human cell lines. *Biochem J* 266: 213–219, 1990. doi:10.1042/bj2660213.
37. **Marsh G, Waugh RE.** Quantifying the mechanical properties of the endothelial glycocalyx with atomic force microscopy. *J Vis Exp* 72: e50163, 2013. doi:10.3791/50163.
38. **Matouk CC, Marsden PA.** Epigenetic regulation of vascular endothelial gene expression. *Circ Res* 102: 873–887, 2008. doi:10.1161/CIRCRESAHA.107.171025.
39. **Moon JJ, Matsumoto M, Patel S, Lee L, Guan JL, Li S.** Role of cell surface heparan sulfate proteoglycans in endothelial cell migration and mechanotransduction. *J Cell Physiol* 203: 166–176, 2005. doi:10.1002/jcp.20220.
40. **Nieuwdorp M, Mooij HL, Kroon J, Atasever B, Spaan JA, Ince C, Holleman F, Diamant M, Heine RJ, Hoekstra JB, Kastelein JJ, Stroes ES, Vink H.** Endothelial glycocalyx damage coincides with microalbuminuria in type 1 diabetes. *Diabetes* 55: 1127–1132, 2006. doi:10.2337/diabetes.55.04.06.db05-1619.
41. **Niu Y, DesMarais TL, Tong Z, Yao Y, Costa M.** Oxidative stress alters global histone modification and DNA methylation. *Free Radic Biol Med* 82: 22–28, 2015. doi:10.1016/j.freeradbiomed.2015.01.028.
42. **Noh H, Oh EY, Seo JY, Yu MR, Kim YO, Ha H, Lee HB.** Histone deacetylase-2 is a key regulator of diabetes- and transforming growth factor-beta1-induced renal injury. *Am J Physiol Renal Physiol* 297: F729–F739, 2009. doi:10.1152/ajprenal.00086.2009.
43. **O'Callaghan R, Job KM, Dull RO, Hlady V.** Stiffness and heterogeneity of the pulmonary endothelial glycocalyx measured by atomic force microscopy. *Am J Physiol Lung Cell Mol Physiol* 301: L353–L360, 2011. doi:10.1152/ajplung.00342.2010.
44. **Ohashi T, Ishii Y, Ishikawa Y, Matsumoto T, Sato M.** Experimental and numerical analyses of local mechanical properties measured by atomic force microscopy for sheared endothelial cells. *Biomed Mater Eng* 12: 319–327, 2002.
45. **Salmon AH, Ferguson JK, Burford JL, Gevorgyan H, Nakano D, Harper SJ, Bates DO, Peti-Peterdi J.** Loss of the endothelial glycocalyx links albuminuria and vascular dysfunction. *J Am Soc Nephrol* 23: 1339–1350, 2012. doi:10.1681/ASN.2012010017.
46. **Sawa H, Murakami H, Ohshima Y, Murakami M, Yamazaki I, Tamura Y, Mima T, Satone A, Ide W, Hashimoto I, Kamada H.** Histone deacetylase inhibitors such as sodium butyrate and trichostatin A inhibit vascular endothelial growth factor (VEGF) secretion from human glioblastoma cells. *Brain Tumor Pathol* 19: 77–81, 2002. doi:10.1007/BF02478931.
47. **Schneider CA, Rasband WS, Eliceiri KW.** NIH Image to ImageJ: 25 years of image analysis. *Nat Methods* 9: 671–675, 2012. doi:10.1038/nmeth.2089.
48. **Shi H, Chen L, Wang H, Zhu S, Dong C, Webster KA, Wei J.** Synergistic induction of miR-126 by hypoxia and HDAC inhibitors in cardiac myocytes. *Biochem Biophys Res Commun* 430: 827–832, 2013. doi:10.1016/j.bbrc.2012.11.061.
49. **Singh A, Ramnath RD, Foster RR, Wylie EC, Fridén V, Dasgupta I, Haraldsson B, Welsh GI, Mathieson PW, Satchell SC.** Reactive oxygen species modulate the barrier function of the human glomerular endothelial glycocalyx. *PLoS One* 8: e55852, 2013. doi:10.1371/journal.pone.0055852.
50. **Thomas AL, Steward WP.** Marimastat: the clinical development of a matrix metalloproteinase inhibitor. *Expert Opin Investig Drugs* 9: 2913–2922, 2000. doi:10.1517/13543784.9.12.2913.
51. **Sundar IK, Yao H, Rahman I.** Oxidative stress and chromatin remodeling in chronic obstructive pulmonary disease and smoking-related diseases. *Antioxid Redox Signal* 18: 1956–1971, 2013. doi:10.1089/ars.2012.4863.
52. **Takahashi K, Tatsunami R, Oba T, Tampo Y.** Buthionine sulfoximine promotes methylglyoxal-induced apoptotic cell death and oxidative stress in endothelial cells. *Biol Pharm Bull* 33: 556–560, 2010. doi:10.1248/bpb.33.556.
53. **Takahashi R, Negishi K, Watanabe A, Arai M, Naganuma F, Ohyama Y, Kurabayashi M.** Serum syndecan-4 is a novel biomarker for patients with chronic heart failure. *J Cardiol* 57: 325–332, 2011. doi:10.1016/j.jjcc.2011.01.012.
54. **Titushkin I, Cho M.** Regulation of cell cytoskeleton and membrane mechanics by electric field: role of linker proteins. *Biophys J* 96: 717–728, 2009. doi:10.1016/j.bpj.2008.09.035.
55. **Vargas-Pinto R, Gong H, Vahabikashi A, Johnson M.** The effect of the endothelial cell cortex on atomic force microscopy measurements. *Biophys J* 105: 300–309, 2013. doi:10.1016/j.bpj.2013.05.034.
56. **Visse R, Nagase H.** Matrix metalloproteinases and tissue inhibitors of metalloproteinases: structure, function, and biochemistry. *Circ Res* 92: 827–839, 2003. doi:10.1161/01.RES.0000070112.80711.3D.
57. **Wang F, Qi Y, Li X, He W, Fan QX, Zong H.** HDAC inhibitor trichostatin A suppresses esophageal squamous cell carcinoma metastasis through HADC2 reduced MMP-2/9. *Clin Invest Med* 36: E87–E94, 2013. doi:10.25011/cim.v36i2.19571.
58. **Wang Y, Branicky R, Noë A, Hekimi S.** Superoxide dismutases: Dual roles in controlling ROS damage and regulating ROS signaling. *J Cell Biol* 217: 1915–1928, 2018. doi:10.1083/jcb.201708007.
59. **Weinbaum S, Tarbell JM, Damiano ER.** The structure and function of the endothelial glycocalyx layer. *Annu Rev Biomed Eng* 9: 121–167, 2007. doi:10.1146/annurev.bioeng.9.060906.151959.
60. **Wright LH, Menick DR.** A class of their own: exploring the nondeacetylase roles of class IIa HDACs in cardiovascular disease. *Am J Physiol Heart Circ Physiol* 311: H199–H206, 2016. doi:10.1152/ajpheart.00271.2016.
61. **Yoon S, Eom GH.** HDAC and HDAC inhibitor: from cancer to cardiovascular diseases. *Chonnam Med J* 52: 1–11, 2016. doi:10.4068/cmj.2016.52.1.1.
62. **Zeng Y, Adamson RH, Curry FR, Tarbell JM.** Sphingosine-1-phosphate protects endothelial glycocalyx by inhibiting syndecan-1 shedding. *Am J Physiol Heart Circ Physiol* 306: H363–H372, 2014. doi:10.1152/ajpheart.00687.2013.
63. **Zhang L, Zeng M, Fan J, Tarbell JM, Curry FR, Fu BM.** Sphingosine-1-phosphate maintains normal vascular permeability by preserving endothelial surface glycocalyx in intact microvessels. *Microcirculation* 23: 301–310, 2016. doi:10.1111/micc.12278.